AD-A116 396

AD A-116396

TECHNICAL LIBRARY

TECHNICAL REPORT ARLCB-TR-82003

STRESS INTENSITY FACTORS FOR RADIAL CRACKS AT OUTER SURFACE OF A PARTIALLY AUTOFRETTAGED CYLINDER SUBJECTED TO INTERNAL PRESSURE

S. L. Pu

May 1982

US ARMY ARMAMENT RESEARCH AND DEVELOPMENT COMMAND
LARGE CALIBER WEAPON SYSTEMS LABORATORY
BENÉT WEAPONS LABORATORY
WATERVLIET, N. Y. 12189

AMCMS No. 611102H600011

DA Project No. 1L161102AH60

PRON No. 1A2250041A1A

APPROVED FOR PUBLIC RELEASE; DISTRIBUTION UNLIMITED

DISCLAIMER

The findings in this report are not to be construed as an official Department of the Army position unless so designated by other authorized documents.

The use of trade name(s) and/or manufacture(s) does not constitute an official indorsement or approval.

DISPOSITION

Destroy this report when it is no longer needed. Do not return it to the originator.

SECURITY CLASSIFICATION OF THIS PAGE *(When Data Entered)*

REPORT DOCUMENTATION PAGE		READ INSTRUCTIONS BEFORE COMPLETING FORM
1. REPORT NUMBER ARLCB-TR-82003	2. GOVT ACCESSION NO.	3. RECIPIENT'S CATALOG NUMBER
4. TITLE *(and Subtitle)* STRESS INTENSITY FACTORS FOR RADIAL CRACKS AT OUTER SURFACE OF A PARTIALLY AUTOFRETTAGED CYLINDER SUBJECTED TO INTERNAL PRESSURE		5. TYPE OF REPORT & PERIOD COVERED Final 6. PERFORMING ORG. REPORT NUMBER
7. AUTHOR(s) S. L. Pu		8. CONTRACT OR GRANT NUMBER(s)
9. PERFORMING ORGANIZATION NAME AND ADDRESS US Army Armament Research & Development Command Benet Weapons Laboratory, DRDAR-LCB-TL Watervliet, NY 12189		10. PROGRAM ELEMENT, PROJECT, TASK AREA & WORK UNIT NUMBERS AMCMS No. 611102H600011 DA Project No. 1L161102AH60 PRON No. 1A2250041A1A
11. CONTROLLING OFFICE NAME AND ADDRESS US Army Armament Research & Development Command Large Caliber Weapon Systems Laboratory Dover, NJ 07801		12. REPORT DATE May 1982 13. NUMBER OF PAGES 43
14. MONITORING AGENCY NAME & ADDRESS*(if different from Controlling Office)*		15. SECURITY CLASS. *(of this report)* UNCLASSIFIED 15a. DECLASSIFICATION/DOWNGRADING SCHEDULE

16. DISTRIBUTION STATEMENT *(of this Report)*

Approved for public release; distribution unlimited.

17. DISTRIBUTION STATEMENT *(of the abstract entered in Block 20, if different from Report)*

18. SUPPLEMENTARY NOTES

19. KEY WORDS *(Continue on reverse side if necessary and identify by block number)*

Stress Intensity Factors
Thick-Wall Cylinder
Multiple Exterior Cracks
Fracture Mechanics
Autofrettaged Cylinder
Finite Elements
Functional Intensity factors

20. ABSTRACT *(Continue on reverse side if necessary and identify by block number)*

The functional stress intensity factor approach which combines the finite element, thermal simulation and weight function methods developed for the computation of stress intensity factors for multiple-radial cracks at the inner surface of a partially autofrettaged cylinder is applied in this report to external cracks. Numerical results of stress intensity factors are obtained for a cylinder with outer diameter twice the inner diameter.

(CONT'D ON REVERSE)

DD FORM 1 JAN 73 1473 EDITION OF 1 NOV 65 IS OBSOLETE

UNCLASSIFIED

SECURITY CLASSIFICATION OF THIS PAGE *(When Data Entered)*

20. ABSTRACT (CONT'D)

A slight decrease in the degree of autofrettage will increase stress intensity factors of inner cracks slightly but will decrease stress intensity factors of external cracks considerably. As in the inner crack case, the cylinder with two diametrically opposed external cracks is in general the weakest configuration and for more than two cracks, the stress intensity factor decreases as the number of external cracks increases.

TABLE OF CONTENTS

TABLES

Page

LIST OF ILLUSTRATIONS

NOMENCLATURE

a	inner radius, used as length unit in this analysis, $a = 1$
b	diameter ratio or normalized outer radius
c	normalized depth of cracks
E	Young's modulus of the tube material, 30×10^6 psi
K	opening mode stress intensity factors (SIF)
$K(p_o), K(p_i)$	SIF due to uniform tension p_o and internal pressure p_i
K_c	SIF due to crack face loading p_c
$K_c(p), K_c(pr^{-2})$	SIF due to $p_c = p$, $p_c = pr^{-2}$, respectively
$K_c(\varepsilon=0.9)$	SIF due to p_c corresponding to a 90 percent overstrain residual stress
N	number of radial cracks
r, θ	polar coordinates centered at the center of the tube
r_c	radius to the tip of an OD crack, $r_c = b - c$
t	wall thickness of the cylinder, $t = b - 1$
T, T_o, T_ρ	temperature at r, $r = a$ and $r = \rho$, respectively
α	linear thermal expansion coefficient, 6.8×10^{-6} in./in./°F
ε	percentage of overstrain, $\varepsilon = (\rho-1)/t$, $0 \leq \varepsilon \leq 1$
ν	Poisson's ratio, 0.3
ρ	radius of elastic-plastic interface during pressurization
σ_o	uniaxial yield stress of the tube material, 170 Ksi
σ_r, σ_θ	normal stress in the radial and tangential direction, respectively

INTRODUCTION

An analytic method is not available for the computation of stress intensity factors for multiple-radial cracks emanating from the bore of a thick-wall cylinder. The computation must depend on various numerical methods. The finite element method, using 12-node quadrilateral, isoparametric elements, has been used to obtain reasonably accurate results for a uniform array of equal depth radial cracks near the bore of a thick-wall cylinder subjected to internal pressure.[1] It is common practice to autofrettage a cylinder so a compressive tangential stress is introduced near the bore. This compressive residual stress reduces the tensile stress near the bore caused by bore pressure. It increases the maximum internal pressure a cylinder can contain elastically, and extends the fatigue life. The residual stress causes added difficulties in computing stress intensity factors. The thermal simulation method[2] is used to simulate the autofrettage residual stress by an active thermal load. The combination of weight function method and the finite element method developed in reference 3 is used to facilitate the numerical computations for various degrees of autofrettage.

---

[1]Pu, S. L. and Hussain, M. A., "Stress Intensity Factors for a Circular Ring With Uniform Array of Radial Cracks Using Cubic Isoparametric Singular Elements," Fracture Mechanics, ASTM STP 677, 1979, pp. 685-699.

[2]Hussain, M. A., Pu, S. L., Vasilakis, J. D., and O'Hara, P., "Simulation of Partial Autofrettage by Thermal Loads," Journal of Pressure Vessel Technology, Vol. 102, No. 3, 1980, pp. 314-318.

[3]Pu, S. L. and Hussain, M. A., "Stress Intensity Factors for Radial Cracks in a Partially Autofrettaged Thick-Wall Cylinder," Presented at the Fourteenth National Symposium on Fracture Mechanics, UCLA, Los Angeles, 1981 and published as a Technical Report ARLCB-TR-81027, 1981.

While the autofrettage process produces favorable compressive residual stress near the bore, it also yields a tensile residual stress near the outer cylindrical surface. This tensile stress, in addition to the tensile stress produced by a bore pressure, causes a high level of stress that may enhance crack initiation or propagation from the outer surface of the cylinder. The problem of an externally cracked, thick-wall cylinder subjected to an internal pressure has been studied by Kapp[4] using the finite element method and by Tracy[5] using the modified mapping collocation method. The K solution for a partially autofrettaged cylinder with external cracks was obtained recently by Parker.[6] The purpose of this report is to extend the method of functional stress intensity factor recently developed in reference 3 for internally cracked cylinders to externally cracked, partially autofrettaged, thick-walled cylinders.

Since an application of this study to gun barrels, some basic differences are noted between ID and OD cracks in cannon tubes. A large number of ID cracks appears after only a few rounds of firing due to heat crazing. The number of OD cracks is far less. The growth of an ID crack tends to drive the

---

[3]Pu, S. L. and Hussain, M. A., "Stress Intensity Factors for Radial Cracks in a Partially Autofrettaged Thick-Wall Cylinder," Presented at the Fourteenth National Symposium on Fracture Mechanics, UCLA, Los Angeles, 1981 and published as a Technical Report ARLCB-TR-81027, 1981.

[4]Kapp, J. A. and Eisenstadt, R., "Crack Growth in Externally Flawed, Autofrettaged Thick-Walled Cylinders and Rings," Fracture Mechanics, ASTM STP 677, 1979, pp. 746-756.

[5]Tracy, P. G., "Elastic Analysis of Radial Cracks Emanating From the Outer and Inner Surfaces of a Circular Ring," Engineering Fracture Mechanics, Vol. 11, 1979, pp. 291-300.

[6]Parker, A. P., "Stress Intensity and Fatigue Crack Growth in Multiply-Cracked, Pressurized, Partially Autofrettaged Thick Cylinders," AMMRC TR81-37, 1981.

crack tip away from the favorable compressive tangential stress field while the growth of an OD crack leads the crack tip inward into the compressive zone of an autofrettaged cylinder. Therefore, the numerical evaluation of K for OD cracks will be limited in this report to a small number of cracks with a crack depth relatively small so that the crack tip remains in the tensile stress field.

FINITE ELEMENT METHOD

In the past decade various finite element techniques have been developed to successfully treat the singular stress field associated with cracks. The use of high order elements is favored because of high degree of accuracy obtainable with a small number of elements. This prompted us to choose 12-node quadrilateral, isoparametric elements for the solution of the problem of multiple-radial cracks in a thick-wall cylinder. A special collapsed triangular element[7] was developed for linear elastic fracture mechanics analysis. No sooner had the 12-node quadrilateral, isoparametric elements and the special crack tip elements been implemented in the general purpose NASTRAN program than we found the special computer program APES (Axisymmetric/Planar Elastic Structures), developed by Gifford.[8] The APES program was written specifically for the use of the 12-node quadrilateral, isoparametric elements. It is a user oriented program and is, in fact, very easy to use. APES consists of two types of crack tip elements for linear elastic fracture

---

[7]Pu, S. L. and Hussain, M. A., "The Collapsed Cubic Isoparametric Element as a Singular Element for Crack Problems," International Journal of Numerical Methods in Engineering, Vol. 12, 1978, pp. 1727-1742.

[8]Gifford, L. N., Jr., "APES-Second Generation Two-Dimensional Fracture Mechanics and Stress Analysis by Finite Elements," DTNSRDC Report 4799, 1975.

analysis. The "enriched" element is deemed better than the "core" crack tip element. We have implemented the newly found collapsed triangular elements into APES as another option for treating linear fracture structures. Both enriched elements and collapsed triangular elements yield comparably accurate results for stress intensity factors. However, the accuracy loss due to distortion in isoparametric finite elements[9,10] should be considered in choosing particular crack tip elements in setting up the finite element idealization for a given geometrical configuration. The collapsed elements were used in reference 1. The accuracy of the results was good in general except several values suffered accuracy loss due to excessive distortion. The enriched elements were used in reference 3 for interior cracks in a partially autofrettaged cylinder. Table I shows a good agreement between the finite element results[3] and the modified mapping collocation results of Tracy[5] for non-autofrettaged cylinders. A similar agreement between results of these two methods for fully autofrettaged cases is shown in Table II. The modified mapping collocation results in Table II were obtained from data supplied by

---

[1]Pu, S. L. and Hussain, M. A., "Stress Intensity Factors for a Circular Ring With Uniform Array of Radial Cracks Using Cubic Isoparametric Singular Elements," Fracture Mechanics, ASTM STP 677, 1979, pp. 685-699.

[3]Pu, S. L. and Hussain, M. A., "Stress Intensity Factors for Radial Cracks in a Partially Autofrettaged Thick-Wall Cylinder," Presented at the Fourteenth National Symposium on Fracture Mechanics, UCLA, Los Angeles, 1981 and published as a Technical Report ARLCB-TR-81027, 1981.

[5]Tracy, P. G., "Elastic Analysis of Radial Cracks Emanating From the Outer and Inner Surfaces of a Circular Ring," Engineering Fracture Mechanics, Vol. 11, 1979, pp. 291-300.

[9]Hopkins, D. A. and Gifford, L. N., "Accuracy Loss in Distorted Isoparametric Finite Elements," DTNSRDC Structures Department Report M2, 1978.

[10]Sickles, J. B. and Gifford, L. N., "A Further Study of Accuracy Loss in Distorted Isoparametric Finite Elements," DTNSRDC Structures Department Report M-50, 1979.

Parker[11] multiplied by the factor $(2/\sqrt{3})$ which converts a result in Tresca's yield criterion to a corresponding result in von Mises' criterion. Due to the success in obtaining accurate results for the case of inner cracks, the enriched elements were again used in this report for multiple cracks emanating from the outer surface. Figure 1(a) shows a typical finite element idealization. For a very shallow crack, the slight modifications in finite element meshes are shown in Figure 1(b).

TABLE I. COMPARISON OF $K_1/p_i\sqrt{\pi c}$ FOR ID CRACKS IN A CYLINDER OF b/a = 2, SUBJECT TO BORE PRESSURE p_i. FINITE ELEMENT[3] VS. MODIFIED MAPPING COLLOCATION (TRACY[5]).

	1 Crack		2 Cracks		4 Cracks	
C	FE	MMC	FE	MMC	FE	MMC
0.1	2.83	2.80	2.87	2.83	2.83	2.75
0.2	2.83	2.77	3.01	2.96	2.78	2.75
0.3	2.89	2.88	3.28	3.23	2.83	2.77
0.4	3.02	2.99	3.56	3.55	2.95	2.99
0.5	3.19	3.15	4.00	4.00	3.15	3.15*

*This value is based on $H_1 = 1.18$ in a private communication prior to the publication of reference 5. The value $H_1 = 1.31$ in reference 5 is probably a typographic error.

---

[3]Pu, S. L. and Hussain, M. A., "Stress Intensity Factors for Radial Cracks in a Partially Autofrettaged Thick-Wall Cylinder," Presented at the Fourteenth National Symposium on Fracture Mechanics, UCLA, Los Angeles, 1981 and published as a Technical Report ARLCB-TR-81027, 1981.

[5]Tracy, P. G., "Elastic Analysis of Radial Cracks Emanating From the Outer and Inner Surfaces of a Circular Ring," Engineering Fracture Mechanics, Vol. 11, 1979, pp. 291-300.

[11]Parker, A. P. and Andrasic, C. P., "Stress Intensity Prediction For a Multiply-Cracked, Pressurized Gun Tube With Residual and Thermal Stresses," Army Symposium on Solid Mechanics 1980 and supplemental data supplied in private communications, 1981.

TABLE II. COMPARISON OF $K_1/-\sigma_o\sqrt{\pi c}$ FOR ID CRACKS IN A FULLY AUTOFRETTAGED CYLINDER OF b/a = 2. FINITE ELEMENT[3] VS. MODIFIED MAPPING COLLOCATION* (PARKER[11]).

	4 Cracks		6 Cracks		10 Cracks		40 Cracks	
C	FE	MMC	FE	MMC	FE	MMC	FE	MMC
0.05	0.981	0.967	0.975	0.959	0.957	0.941	0.659	0.670
0.1	0.895	0.871	0.871	0.847	0.817	0.794	0.442	0.432
0.2	0.745	0.722	0.684	0.662	0.575	0.557	0.277	0.271
0.3	0.628	0.609	0.539	0.521	0.417	0.403	0.197	0.191

*MMC results were supplied by Parker in a private communication then multiplied by $2/\sqrt{3}$ to convert from Tresca yield criterion to von Mises' criterion.

THERMAL SIMULATION

In a partially autofrettaged tube, the plane-strain residual stresses based on von Mises' yield criterion for an incompressible material are given by[12]

$$\sigma_r(r) = \begin{cases} \frac{\sigma_o}{\sqrt{3}} \{(2 \log \frac{r}{\rho} - 1 + \frac{\rho^2}{b^2}) - P_1(\frac{1}{b^2} - \frac{1}{r^2})\} & 1 \leq r \leq \rho \quad (1) \\ \frac{\sigma_o}{\sqrt{3}} (\rho^2 - P_1)(\frac{1}{b^2} - \frac{1}{r^2}) & \rho \leq r \leq b \quad (2) \end{cases}$$

---

[3]Pu, S. L. and Hussain, M. A., "Stress Intensity Factors for Radial Cracks in a Partially Autofrettaged Thick-Wall Cylinder," Presented at the Fourteenth National Symposium on Fracture Mechanics, UCLA, Los Angeles, 1981 and published as a Technical Report ARLCB-TR-81027, 1981.

[11]Parker, A. P. and Andrasic, C. P., "Stress Intensity Prediction For a Multiply-Cracked, Pressurized Gun Tube With Residual and Thermal Stresses," Army Symposium on Solid Mechanics 1980 and supplemental data supplied in private communications, 1981.

[12]Hill, R., The Mathematical Theory of Plasticity, Oxford at the Clarendon Press, 1950.

$$\sigma_\theta(r) = \begin{cases} \frac{\sigma_o}{\sqrt{3}} \{2 \log \frac{r}{\rho} + 1 + \frac{\rho^2}{b^2} - P_1(\frac{1}{b^2} + \frac{1}{r^2})\} & 1 \leq r \leq \rho \quad (3) \\ \frac{\sigma_o}{\sqrt{3}} (\rho^2 - P_1)(\frac{1}{b^2} + \frac{1}{r^2}) & \rho \leq r \leq b \quad (4) \end{cases}$$

where

$$P_1 = P_1(\rho) = \frac{b^2}{b^2-1} (1 - \frac{\rho^2}{b^2} + 2 \log \rho) \quad (5)$$

In this residual stress field, the presence of a sharp crack or a notch may cause geometric changes of the cylinder and redistribution of stresses. The stress redistribution in case of a notch and the stress intensity factor in case of a sharp crack can not be directly formulated as a boundary value problem for finite element application. It is verified in reference 2 that the following thermal stresses are present in a thick-wall cylinder

$$\sigma_r(r) = \begin{cases} \frac{E\alpha(T_o - T_\rho)}{2(1-\nu)\log \rho} \{(2 \log \frac{r}{\rho} - 1 + \frac{\rho^2}{b^2}) - P_1(\frac{1}{b^2} - \frac{1}{r^2})\} & 1 \leq r \leq \rho \quad (6) \\ \frac{E\alpha(T_o - T_\rho)}{2(1-\nu)\log \rho} (\rho^2 - P_1)(\frac{1}{b^2} - \frac{1}{r^2}) & \rho \leq r \leq b \quad (7) \end{cases}$$

$$\sigma_\theta(r) = \begin{cases} \frac{E\alpha(T_o - T_\rho)}{2(1-\nu)\log \rho} \{2 \log \frac{r}{\rho} + 1 + \frac{\rho^2}{b^2} - P_1(\frac{1}{b^2} + \frac{1}{r^2})\} & 1 \leq r \leq \rho \quad (8) \\ \frac{E\alpha(T_o - T_\rho)}{2(1-\nu)\log \rho} (\rho^2 - P_1)(\frac{1}{\rho^2} + \frac{1}{r^2}) & \rho \leq r \leq b \quad (9) \end{cases}$$

---

[2]Hussain, M. A., Pu, S. L., Vasilakis, J. D., and O'Hara, P., "Simulation of Partial Autofrettage by Thermal Loads," Journal of Pressure Vessel Technology, Vol. 102, No. 3, 1980, pp. 314-318.

if the cylinder is subjected to the thermal load

$$T(r) = \begin{cases} T_o - \dfrac{(T_o - T_\rho)}{\log \rho} \log r & 1 \leq r \leq \rho \\ T_\rho & \rho \leq r \leq b \end{cases} \tag{10}$$

The thermal stresses and the residual stresses become equivalent if the temperature gradient of the thermal load and the material properties of the cylinder satisfy the following relation

$$T_o - T_\rho = \frac{4(1-\nu)\sigma_o}{\sqrt{3}\, E\alpha} \log \rho \tag{11}$$

where σ_o is the uniaxial yield stress and T_o or T_ρ may be assigned arbitrarily.

The replacement of residual stresses by an equivalent thermal load provides a method by which the original residual stress problem is transformed into a boundary value problem. The application of the thermal simulation method is illustrated in references 3 and 13. In this report the method of thermal simulation is again used to handle external radial cracks in a residual stress field. Since $r = \rho$ divides the temperature into two distinct fields, it is advisable to use $r = \rho$ as a dividing arc in the finite element idealization to correctly reflect the constant temperature field versus the logarithmically varying field.

---

[3] Pu, S. L. and Hussain, M. A., "Stress Intensity Factors for Radial Cracks in a Partially Autofrettaged Thick-Wall Cylinder," Presented at the Fourteenth National Symposium on Fracture Mechanics, UCLA, Los Angeles, 1981 and published as a Technical Report, ARLCB-TR-81027, 1981.

[13] Pu, S. L. and Hussain, M. A., "Residual Stress Redistribution Caused by Notches and Cracks in a Partially Autofrettaged Tube," Journal of Pressure Vessel Technology, Vol. 103, No. 4, 1981, pp. 301-306.

WEIGHT FUNCTION AND FUNCTIONAL INTENSITY FOR EXTERIOR CRACKS

The finite element and the thermal simulation methods enable us to compute stress intensity factors for cracks in a cylinder subjected to an internal pressure and autofrettage residual stresses. A combination of these methods and the weight function method is developed in reference 3. For a given crack geometry, only three finite element computations are needed for the three types of loadings applied separately. These loadings are (a) bore pressure p_i (not on crack face), (b) uniform tension p_o on OD and, (c) a thermal load simulating the 100 percent overstrain residual stresses. These values of stress intensity factors are denoted by $K(p_i)$, $K(p_o)$, and $K(\varepsilon=1)$. Functional stress intensity factors are defined as $K_c(1)$, $K_c(r^{-2})$, and $K_c(\log r)$ and can be solved algebraically from $K(p_i)$, $K(p_o)$, and $K(\varepsilon=1)$. The stress intensity factor for the same crack geometry due to a partial autofrettage residual stress is given by a simple algebraic equation in terms of the functional stress intensity factors. The method used for internal cracks in reference 3 can be equally applied to external cracks. The expressions for external cracks given below are slightly different from those given in reference 3 for internal cracks.

According to Bueckner[14] and Rice,[15] a weight function is a universal function which depends only on geometry and not on loadings. If the stress

---

[3]Pu, S. L. and Hussain, M. A., "Stress Intensity Factors For Radial Cracks in a Partially Autofrettaged Thick-Wall Cylinder," Presented at the Fourteenth National Symposium on Fracture Mechanics, UCLA, Los Angeles 1981 and published as a Technical Report ARLCB-TR-81027, 1981.

[14]Bueckner, H. F., "A Novel Principle for the Computation of Stress Intensity Factors," Z. Agnew Math. Mech., Vol. 50, 1970, pp. 529-546.

[15]Rice, J. R., "Some Remarks on Elastic Crack-Tip Stress Fields," Int. Journal of Solids and Structures, Vol. 8, 1972, pp. 751-758.

intensity factor $K^{(1)}$ and displacement field $\underset{\sim}{u}^{(1)}$ associated with load system 1 are known, the weight function for the cracked geometry is

$$\underset{\sim}{h} = \frac{H}{2K^{(1)}(c)} \frac{\partial u^{(1)}(x,y,c)}{\partial c} \tag{12}$$

where $H = E$ for plane stress and $H = E/(1-\nu^2)$ for plane strain. Once h is determined, the stress intensity factor induced by any other symmetric load system $\underset{\sim}{t}$ and $\underset{\sim}{f}$ is given by

$$K = \int_{\Gamma} \underset{\sim}{t} \cdot \underset{\sim}{h} \, d\Gamma + \int_{A} \underset{\sim}{f} \cdot \underset{\sim}{h} \, dA \tag{13}$$

where $\underset{\sim}{t}$ is the stress vector acting on boundary Γ around the crack tip and $\underset{\sim}{f}$ is the body force in region A defined by Γ. For our radial cracks in a cylinder, $\underset{\sim}{f} = 0$ is used and equation (13) can be reduced to

$$K = \frac{H}{K^*} \int_{o}^{c} p_c(x) \frac{\partial v}{\partial c} \, dx \tag{14}$$

where c is the crack depth and x is a distance both measured from the outer cylindrical surface with x and r related by

$$x = b - r \tag{15}$$

K^* and v are the stress intensity factor and the crack opening displacement associated with a certain loading, while K is the stress intensity factor for the applied symmetric loading and $p_c(x)$ is the equivalent crack face loading reduced from the applied loads by superposition of a solution for a crack-free body under the same loads.

For a uniform tension p_o on the OD and an internal pressure p_i (note p_o or p_i not acting on crack faces), the equivalent crack face loadings are respectively

$$p_c(x) = \frac{b^2 p_o}{b^2-1}\left[1 + (b-x)^{-2}\right] \tag{16}$$

$$p_c(x) = \frac{p_i}{b^2-1}\left[1 + b^2(b-x)^{-2}\right] \tag{17}$$

The crack face loading equivalent to a 100 percent autofrettage residual stress is

$$p_c(x) = \frac{\sigma_o}{\sqrt{3}}\left[\{2 - P_1(b)\} - P_1(b)(b-x)^{-2} + 2\log(b-x)\right] \tag{18}$$

Substituting into equation (14) from equations (16), (17), and (18) we have

$$\frac{K(p_o)}{p_o\sqrt{\pi c}} = \frac{b^2}{b^2-1}\frac{K_c(1)}{\sqrt{\pi c}} + \frac{b^2}{b^2-1}\frac{K_c(r^{-2})}{\sqrt{\pi c}} \tag{19}$$

$$\frac{K(p_i)}{p_i\sqrt{\pi c}} = \frac{1}{b^2-1}\frac{K_c(1)}{\sqrt{\pi c}} + \frac{b^2}{b^2-1}\frac{K_c(r^{-2})}{\sqrt{\pi c}} \tag{20}$$

$$\frac{K_c(\varepsilon=1)}{\sigma_o\sqrt{\pi c}} = \frac{1}{\sqrt{3\pi c}}\left[\{2 - P_1(b)\}K_c(1) - P_1(b)K_c(r^{-2}) + 2K_c(\log r)\right] \tag{21}$$

where the functional intensity factors are defined by

$$K_c(1) = \frac{H}{K^*}\int_o^c \frac{\partial v}{\partial c}\,dx \tag{22}$$

$$K_c(r^{-2}) = \frac{H}{K^*}\int_o^c (b-x)^{-2}\frac{\partial v}{\partial c}\,dx \tag{23}$$

$$K_c(\log r) = \frac{H}{K^*}\int_o^c [\log(b-x)]\frac{\partial v}{\partial c}\,dx \tag{24}$$

For a given crack configuration, we can solve for these functional intensity factors from equations (19) to (21) with the left hand sides of these equations known from finite element computations. Once the functional intensity factors are known, it is a simple matter to compute stress intensity

factors for the same crack due to residual stresses corresponding to a partial autofrettage, provided that OD cracks are in the region beyond r = ρ. The tangential residual stress in this region is

$$\sigma_\theta(x) = \frac{\sigma_o}{\sqrt{3}} [\rho^2 - P_1(\rho)][b^{-2} + (b-x)^{-2}] \ , \quad 0 < x < (1-\varepsilon)t \tag{25}$$

Using Eq. (25) as the crack face loading in equation (14), we have

$$\frac{K_c(\varepsilon)}{\sigma_o\sqrt{\pi c}} = \frac{1}{\sqrt{3}} [\frac{\rho^2 - P_1(\rho)}{b^2}][\frac{K_c(1)}{\sqrt{\pi c}} + b^2 \frac{K_c(r^{-2})}{\sqrt{\pi c}}] \ , \quad c \leq (1-\varepsilon)t \tag{26}$$

Comparing equation (26) with equation (20) we can write

$$\frac{K_c(\varepsilon)}{\sigma_o\sqrt{\pi c}} = \frac{1}{\sqrt{3}} (\rho^2 - 1 - 2 \log \rho) \frac{K(p_i)}{p_i\sqrt{\pi c}} \tag{27}$$

It is clear that the stress intensity factor due to partial autofrettage residual stress is a multiplication factor, depending on degree of autofrettage, times the stress intensity factor due to internal pressure. This was also observed by Parker.[11]

In case the crack tip depth c is larger than (1-ε)t, the crack face loading must be expressed in the form

$$p_c(x) = \begin{cases} \frac{\sigma_o}{\sqrt{3}} [\rho^2 - P_1(\rho)][b^{-2} + (b-x)^{-2}] & 0 \leq x \leq (1-\varepsilon)t \quad (28a) \\ \frac{\sigma_o}{\sqrt{3}} [\{2 - P_1(\rho)\} - P_1(\rho)(b-x)^{-2} + 2 \log(b-x)] & (1-\varepsilon)t \leq x \leq t \quad (28b) \end{cases}$$

---

[11] Parker, A. P. and Andrasic, C. P., "Stress Intensity Prediction For a Multiply-Cracked, Pressurized Gun Tube With Residual and Thermal Stresses," Army Symposium on Solid Mechanics 1980 and supplemental data supplied in private communications, 1981.

In this case neither equation (26) nor (27) is valid. However, if $c/t = 1 - \varepsilon + \delta$ and δ is small, we may use equation (26) or (27) to obtain an approximate stress intensity factor. The final stress intensity factor is the sum of the approximate and a correction K_δ. The correction stress intensity factor K_δ is calculated from

$$\frac{K_\delta}{\sigma_o\sqrt{\pi c}} = \frac{1}{\sqrt{3\pi c}} \frac{H}{K^*} \int_{(1-\varepsilon)t}^{(1-\varepsilon+\delta)t} p_c(x) \frac{\partial v}{\partial c}\, dx \qquad (29)$$

where $p_c(x)$ is the difference between equations (28b) and (28a) or

$$p_c(x) = (1-2 \log \rho) - \rho^2(b-x)^{-2} + 2 \log(b-x) \qquad (30)$$

and v is an approximation based on the crack face displacement of Westergaard near field solution

$$v(\xi) = \frac{2K^*}{H} \left(\frac{2\xi}{\pi}\right)^{1/2} \qquad (31)$$

where ξ is a distance measured from the crack tip outward radially.

Carrying out the integration of equation (29) using equations (30) and (31) we have

$$\frac{K_\delta}{\sigma_o\sqrt{\pi c}} = \frac{1}{\sqrt{3\pi c}} \frac{2}{\pi} \{(1-2 \log \rho)(I_1+I_1') - \rho^2(I_2+I_2') + 2(I_3+I_3')\} \qquad (32)$$

where

$$I_1 = 2\sqrt{\delta t} \quad , \quad I_1' = \frac{2}{3c} (\delta t)^{3/2} \qquad (33)$$

$$I_2 = \frac{1}{r_c} \left[\frac{\sqrt{\delta t}}{\rho} + r_c^{-1/2} \tan^{-1}\sqrt{\delta t/r_c}\right] \qquad (34)$$

$$I_2' = \frac{1}{c} \left[-\frac{\sqrt{\delta t}}{\rho} + r_c^{-1/2} \tan^{-1}\sqrt{\delta t/r_c}\right] \qquad (35)$$

$$I_3 = 2[(-2+\log \rho)\sqrt{\delta t} + 2\sqrt{r_c} \tan^{-1}\sqrt{\delta t/r_c}] \quad (36)$$

$$I_3' = \frac{2}{3c}[(\delta t)^{3/2}\log \rho + \frac{2}{3}(3r_c-\delta t)\sqrt{\delta t} - 2r_c^{3/2} \tan^{-1}\sqrt{\delta t/r_c}] \quad (37)$$

with the abbreviation $r_c = b - c$.

NUMERICAL RESULTS FOR THE CASE OF b = 2, a = 1

Before presenting results for external multiple cracks, several graphs supplement to reference 3 for interior cracks are added here. Figure 2 is stress intensity factor due to residual stresses in a fully autofrettaged cylinder as a function of crack depths for several values of N from 2 to 40. Stress intensity factors are negative due to compressive crack face loadings. Similarly, the ordinates of Figures 5 and 6 of reference 3 should be negative. Figure 3 shows the decrease in stress intensity factor due to an increased degree of autofrettage for a single internal crack.

The stress intensity factor due to combined internal pressure and autofrettage residual stresses, Figure 4, remains highest for two diametrically opposite inner cracks and decreases monotonically as the number of cracks increases for various crack depths and various degrees of autofrettage.

For external multiple cracks, the dimensionless stress intensity factors are shown as a function of crack depths in Figure 5 for a non-autofrettaged cylinder and in Figure 6 for a fully autofrettaged cylinder for several values

---

[3]Pu, S. L. and Hussain, M. A., "Stress Intensity Factors for Radial Cracks in a Partially Autofrettaged Thick-Wall Cylinder," Presented at the Fourteenth National Symposium on Fracture Mechanics, UCLA, Los Angeles, 1981 and published as a Technical Report ARLCB-TR-81027, 1981.

of N from 1 to 20. A comparison of our finite element results with Tracy's modified mapping collocation results[5] is given in Table III for cracks emanating from the outer surface of a non-autofrettaged cylinder subjected to an internal pressure. The agreement is not as good as shown in Table I for cracks near the inner surface. Previous finite element results were, in general, higher than MMC results in Table I, but the opposite appears in Table III. The finite element results using 8-node quadratic quadrilateral elements with collapsed triangles as singular crack tip elements for one external crack in a non-autofrettaged cylinder subjected to internal pressure given by Kapp[4] are also shown in Table III. Better agreement is seen between references 4 and 5. This suggests an idealization with more refined elements than used in Figure 1 may be needed for better accuracy for external cracks. To demonstrate the method it is deemed enough to use the coarse meshes of Figure 1. For partially autofrettaged cylinders Parker's results[11] are based on results of non-autofrettaged cylinders.[5] The agreement between finite element and modified mapping collocation for an autofrettaged case can only be expected to be as good as that for the non-autofrettaged case.

---

[4]Kapp, J. A. and Eisenstadt, R., "Crack Growth in Externally Flawed, Autofrettaged Thick-Walled Cylinders and Rings," Fracture Mechanics, ASTM STP 677, 1979, pp. 746-756.

[5]Tracy, P. G., "Elastic Analysis of Radial Cracks Emanating From the Outer and Inner Surfaces of a Circular Ring," Engineering Fracture Mechanics, Vol. 11, 1979, pp. 291-300.

[11]Parker, A. P. and Andrasic, C. P., "Stress Intensity Prediction for a Multiply-Cracked, Pressurized Gun Tube With Residual and Thermal Stresses," Army Symposium on Solid Mechanics 1980 and supplemental data supplied in private communications, 1981.

TABLE III. COMPARISON OF $K_I/p_i\sqrt{\pi c}$ FOR OD CRACKS IN A CYLINDER OF b/a = 2 SUBJECTED TO A BORE PRESSURE p_i. FINITE ELEMENT (THIS STUDY) VS. MODIFIED MAPPING COLLOCATION (TRACY[5]).

	1 Crack			2 Cracks		3 Cracks		4 Cracks	
c	FE	FE[4]	MMC	FE	MMC	FE	MMC	FE	MMC
0.1	0.756	0.806	0.800	0.758	0.813	0.753	0.807	0.747	0.807
0.2	0.838	0.917	0.913	0.846	0.913	0.830	0.880	0.802	0.867
0.3	0.960	1.056	1.04	0.977	1.06	0.922	1.00	0.874	0.947

Functional stress intensity factors are obtained using equations (19), (20), and (21), and the results are plotted in Figures 7, 8, and 9. These results are the basis for the computation of stress intensity factors for multiple exterior cracks for various degrees of autofrettage. For example, given N = 4, readings taken from Figures 7 and 8 are $K_c(p)/(p\sqrt{\pi c}) = 1.12$ and $K_c(pr^{-2})/(p\sqrt{\pi c}) = 0.320$ for c/t = 0.2 and $K_c(p)/(p\sqrt{\pi c}) = 1.18$, $K_c(pr^{-2})/(p\sqrt{\pi c}) = 0.360$ for c/t = 0.3. For $\varepsilon = 0.8$, the stress intensity factor due to the autofrettage residual stress can be computed from equation (26) which gives $K(\varepsilon=0.8)/(\sigma_o\sqrt{\pi c}) = 0.492$ for c/t = 0.2. If equation (27) is used, $K(p_i)/(p_i\sqrt{\pi c})$ and the multiplication factors are 0.802 and 0.615 respectively, then $K(\varepsilon=0.8)/(\sigma_o\sqrt{\pi c}) = 0.493$. For c/t = 0.3, the crack tip enters the region $r \leq 1.8$ (inside the elastic-plastic radius). Equation (26) gives an

[5]Tracy, P. G., "Elastic Analysis of Radial Cracks Emanating From the Outer and Inner Surfaces of a Circular Ring," Engineering Fracture Mechanics, Vol. 11, 1979, pp. 291-300.

approximate value, $K(\varepsilon=0.8)/(\sigma_o\sqrt{\pi c}) = 0.537$. Using equation (32) we compute $K_\delta/(\sigma_o\sqrt{\pi c}) = -0.05$. The final result for $c/t = 0.3$ is $K_c(\varepsilon=0.8)/(\sigma_o\sqrt{\pi c}) = 0.487$. A finite element computation for the case $\varepsilon = 0.8$, $c/t = 0.3$ was performed and the result is $K/(\sigma_o\sqrt{\pi c}) = 0.486$.

The dimensionless stress intensity factor as a function of degree of autofrettage is shown in Figure 10 for selected values of N and c/t. In Figure 11 the same is shown as a function of the c/t for the single crack case for several values of ε. The stress intensity factor drops considerably from the fully autofrettaged condition to a 60 percent or 70 percent autofrettage for small values of c/t. In a similar graph for a shallow interior crack, Figure 3, the stress intensity factor increases slightly from the lowest value corresponding to the fully autofrettaged condition to 60 or 70 percent autofrettage. This suggests that a partially autofrettaged cylinder may sometimes have the advantage over a fully autofrettaged one.

For a combination of residual stresses and internal pressure, the stress intensity factor is simply an algebraic sum. The stress intensity factor normalized by $K_o = \sigma_\theta(r=b)\sqrt{\pi c}$ is shown as a function of c/t in Figure 12 for various combinations of residual stress and internal pressure $p_i = \sigma_o/f$ for the cases of two and twenty cracks. The stress intensity factor normalized by $\sigma_o\sqrt{\pi c}$ is given as a function of N in Figure 13. It is clear that the stress intensity factor is largest for N = 2 under various combinations of residual stresses and internal pressures. The stress intensity factor is monotonically decreasing as the number of cracks increases from N = 2. For shallow cracks, i.e. $c/t \leq 0.1$, the interaction among cracks becomes weak. The stress intensity factor for N = 2 is nearly the same as for N = 1.

APPROXIMATIONS FOR SHALLOW CRACKS

The finite element method has some difficulty in calculating stress intensity factors for very shallow ID or OD cracks due to the small size of crack tip elements required to solve the shallow crack problem. An approximate approach is to extend the graphs of stress intensity factor versus crack depth c to small values of c using the knowledge that the limiting value of $K_c(p_c)/\sqrt{\pi c}$ approaches 1.12 σ_θ as $c \to 0$ where $\sigma_\theta = \sigma_\theta(r=a)$ for inner cracks and $\sigma_\theta = \sigma_\theta(r=b)$ for external cracks. The dotted lines in Figures 7, 8, and 9 represent the extensions. The curves in the region $0 < c/t < 0.05$ in Figures 2, 3, and 4 in reference 3 are also such extensions. Taking readings of functional stress intensity from those graphs and using the method described in this report and in reference 3, we can compute stress intensity factors for various values of c, including small values, for various values of N.

Another approximate method for shallow cracks suggested by Underwood and Throop[16] assumes the crack face loading be linear varying and uses the stress intensity solutions of Bueckner[17] for uniform pressure and Tada[18] and Benthem[19]

---

[3]Pu, S. L. and Hussain, M. A., "Stress Intensity Factors for Radial Cracks in a Partially Autofrettaged Thick-Wall Cylinder," Presented at the Fourteenth National Symposium on Fracture Mechanics, UCLA, Los Angeles, 1981 and published as a Technical Report ARLCB-TR-81027, 1981.

[16]Underwood, J. H. and Throop, J. F., "Surface Crack K-Estimates and Fatigue Life Prediction," ASTM STP 687, 1979, pp. 195-210.

[17]Bueckner, H. F., "Some Stress Singularities and Their Computation by Means of Integral Equations," Boundary Problems in Differential Equations, Ed., R. E. Langer, University of Wisconsin Press, Madison, WI, 1960.

[18]Tada, H., Paris, P. C. and Irwin, G. R., The Stress Analysis of Cracks Handbook, Del Research Corporation, Hellertown, PA, 1973.

[19]Benthem, J. P. and Koiter, W. T., "Asymptotic Approximations to Crack Problems," Methods of Analysis of Crack Problems, Ed., G. C. Sih, Noordhoff International Publishing, 1972.

for linear varying pressure. For a single crack at inner surface the formula is given by

$$K_I = [1.12\ \sigma_\theta(r=a) - 0.68\ \{\sigma_\theta(r=a) - \sigma_\theta(r=r_c)\}]\sqrt{\pi c} \qquad (38)$$

A similar equation for a single crack at outer surface is

$$K_I = [1.12\ \sigma_\theta(r=b) - 0.68\ \{\sigma_\theta(r=b) - \sigma_\theta(r=r_c)\}]\sqrt{\pi c} \qquad (39)$$

These equations give good approximations for more than one crack for small values of c.

We have worked out several examples using both the functional intensity factor approach and the linear varying stress approach and compared the results with available results by other methods. The comparison is given in Table IV for inner cracks and Table V for outer cracks. The agreement between the two approximate approaches is good for small c/t (N may be large). If c/t is not very small and if N is large then the functional intensity approach is better.

TABLE IV. COMPARISON OF K/K_o* FOR SHALLOW ID CRACKS IN A CYLINDER OF b/a = 2 SUBJECTED TO EITHER A BORE PRESSURE p_i OR A RESIDUAL STRESS CORRESPONDING TO $\varepsilon = 1$ OR $\varepsilon = 0.6$.

c/t	Loading	All N Eq. (38)	N = 4 FE[3]	N = 4 MMC[11]	N = 20 FE[3]	N = 18 MMC[11]
0.01	p_i	1.113	1.109	1.106	1.084	1.101
	$\varepsilon = 1$	1.075	1.067	1.068	1.046	1.063
	$\varepsilon = 0.6$	0.927	0.919		0.902	
0.04	p_i	1.094	1.077	1.076	0.980	1.010
	$\varepsilon = 1$	1.011	0.992	0.994	0.907	0.930
	$\varepsilon = 0.6$	0.866	0.848		0.777	
0.10	p_i	1.061	1.058	1.035	0.778	0.796
	$\varepsilon = 1$	0.896	0.892	0.871	0.642	0.657
	$\varepsilon = 0.6$	0.756	0.752		0.539	

*$K_o = \frac{8}{3} p_i \sqrt{\pi c}$ for pressure p_i acting on bore and crack face,

$K_o = \sigma_o \sqrt{\pi c}$ for autofrettage residual stress.

---

[3]Pu, S. L. and Hussain, M. A., "Stress Intensity Factors for Radial Cracks in a Partially Autofrettaged Thick-Wall Cylinder," Presented at the Fourteenth National Symposium on Fracture Mechanics, UCLA, Los Angeles, 1981 and published as a Technical Report ARLCB-TR-81027, 1981.

[11]Parker, A. P. and Andrasic, C. P., "Stress Intensity Prediction for a Multiply-Cracked, Pressurized Gun Tube With Residual and Thermal Stresses," Army Symposium on Solid Mechanics 1980 and supplemental data supplied in private communications, 1981.

TABLE V. COMPARISON OF K/K_o* FOR SHALLOW OD CRACKS IN A CYLINDER OF b/a = 2 SUBJECTED TO EITHER A BORE PRESSURE p_i OR A RESIDUAL STRESS CORRESPONDING TO $\varepsilon = 1$ OR $\varepsilon = 0.6$.

c/t	Loading	Eq. (39) All N	FE (This Study) N = 1	FE (This Study) N = 20	FE[4] N = 1
0.01	p_i	1.123	1.113	1.102	1.124
	$\varepsilon = 1$	0.69	0.68	0.67	
	$\varepsilon = 0.6$	0.265	0.263		
0.04	p_i	1.134	1.104	1.052	1.132
	$\varepsilon = 1$	0.672	0.654	0.608	
	$\varepsilon = 0.6$	0.271	0.263	0.251	
0.1	p_i	1.157	1.128$^{\Delta}$	0.944	1.208
	$\varepsilon = 1$	0.636	0.629	0.525	
	$\varepsilon = 0.6$	0.276	0.269	0.225	

*$K_o = \frac{2}{3} p_i\sqrt{\pi c}$ for bore pressure p_i and $K_o = \sigma_o\sqrt{\pi c}$ for autofrettage residual stress.

$^{\Delta}$MMC result for this case is $K/K_o = 1.20$.[5]

---

[4]Kapp, J. A. and Eisenstadt, R., "Crack Growth in Externally Flawed, Autofrettaged Thick-Walled Cylinders and Rings," Fracture Mechanics, ASTM STP 677, 1979, pp. 746-756.

[5]Tracy, P. G., "Elastic Analysis of Radial Cracks Emanating From the Outer and Inner Surfaces of a Circular Ring," Engineering Fracture Mechanics, Vol. 11, 1979, pp. 291-300.

CONCLUSIONS

The method developed in a previous paper[3] for multiple-radial cracks at the inner surface of an autofrettaged thick-wall cylinder can be applied to multiple cracks at the outer surface of the cylinder with slight modification. A simple modification factor depends on the degree of autofrettage, and can be used to obtain stress intensity factors due to partially autofrettaged residual stress and internal pressure, provided the OD cracks are not beyond the elastic and plastic interface (during the autofrettage pressurization).

The agreement between numerical results from finite element and modified mapping collocation for the exterior crack case is not as good as for interior cracks. In virtue of the results in reference 4, the accuracy of the finite element results using 12-node cubic elements probably can be improved with an idealization consisting of more elements than those used in this study.

As in the case of interior cracks, the cylinder with two diametrically opposed cracks is, in general, the weakest configuration. For more than two cracks, the stress intensity factor decreases as the number of external cracks increases. The autofrettage process will prolong the useful life of a pressure vessel with radial cracks at the inner surface, but will have an adverse effect on radial cracks at the outer surface. If 100 percent autofrettage causes the concern of fracture failure shifted from inner cracks to outer cracks, then the

---

[3]Pu, S. L. and Hussain, M. A., "Stress Intensity Factors for Radial Cracks in a Partially Autofrettaged Thick-Wall Cylinder," Presented at the Fourteenth National Symposium on Fracture Mechanics, UCLA, Los Angeles, 1981 and published as a Technical Report ARLCB-TR-81027, 1981.

[4]Kapp, J. A. and Eisenstadt, R., "Crack Growth in Externally Flawed, Autofrettaged Thick-Walled Cylinders and Rings," Fracture Mechanics, ASTM STP 677, 1979, p. 746-756.

degree of autofrettage should be reduced. A slight decrease in the degree of autofrettage will slightly increase the stress intensity factor at interior cracks, and at the same time will considerably decrease the stress intensity factor at exterior cracks. It is desirable to obtain the optimal degree of autofrettage to best suit the crack configuration and loading.

REFERENCES

1. Pu, S. L. and Hussain, M. A., "Stress Intensity Factors for a Circular Ring With Uniform Array of Radial Cracks Using Cubic Isoparametric Singular Elements," Fracture Mechanics, ASTM STP 677, 1979, pp. 685-699.
2. Hussain, M. A., Pu, S. L., Vasilakis, J. D., and O'Hara, P., "Simulation of Partial Autofrettage by Thermal Loads," Journal of Pressure Vessel Technology, Vol. 102, No. 3, 1980, pp. 314-318.
3. Pu, S. L. and Hussain, M. A., "Stress Intensity Factors for Radial Cracks in a Partially Autofrettaged Thick-Wall Cylinder," Presented at the Fourteenth National Symposium on Fracture Mechanics, UCLA, Los Angeles, 1981 and published as a Technical Report ARLCB-TR-81027, 1981.
4. Kapp, J. A. and Eisenstadt, R., "Crack Growth in Externally Flawed, Autofrettaged Thick-Walled Cylinders and Rings," Fracture Mechanics, ASTM STP 677, 1979, pp. 746-756.
5. Tracy, P. G., "Elastic Analysis of Radial Cracks Emanating From the Outer and Inner Surfaces of a Circular Ring," Engineering Fracture Mechanics, Vol. 11, 1979, pp. 291-300.
6. Parker, A. P., "Stress Intensity and Fatigue Crack Growth in Multiply-Cracked, Pressurized, Partially Autofrettaged Thick Cylinders," AMMRC TR81-37, 1981.
7. Pu, S. L. and Hussain, M. A., "The Collapsed Cubic Isoparametric Element as a Singular Element for Crack Problems," International Journal of Numerical Methods in Engineering, Vol. 12, 1978, pp. 1727-1742.

8. Gifford, L. N. Jr., "APES - Second Generation Two-Dimensional Fracture Mechanics and Stress Analysis by Finite Elements," DTNSRDC Report 4799, 1975.

9. Hopkins, D. A. and Gifford, L. N., "Accuracy Loss in Distorted Isoparametric Finite Elements," DTNSRDC Structures Department Report M2, 1978.

10. Sickles, J. B. and Gifford, L. N., "A Further Study of Accuracy Loss in Distorted Isoparametric Finite Elements," DTNSRDC Structures Department Report M-50, 1979.

11. Parker, A. P. and Andrasic, C. P., "Stress Intensity Prediction For a Multiply-Cracked, Pressurized Gun Tube With Residual and Thermal Stresses," Army Symposium on Solid Mechanics 1980 and supplemental data supplied in private communications, 1981.

12. Hill, R., The Mathematical Theory of Plasticity, Oxford at the Clarendon Press, 1950.

13. Pu, S. L. and Hussain, M. A., "Residual Stress Redistribution Caused by Notches and Cracks in a Partially Autofrettaged Tube," Journal of Pressure Vessel Technology, Vol. 103, No. 4, 1981, pp. 301-306.

14. Bueckner, H. F., "A Novel Principle for the Computation of Stress Intensity Factors," Z. Agnew. Math. Mech., Vol. 50, 1970, pp. 529-546.

15. Rice, J. R., "Some Remarks on Elastic Crack-Tip Stress Fields," Int. Journal of Solids and Structures, Vol. 8, 1972, pp. 751-758.

16. Underwood, J. H. and Throop, J. F., "Surface Crack K-Estimates and Fatigue Life Prediction, " ASTM STP 687, 1979, pp. 195-210.

17. Bueckner, H. F., "Some Stress Singularities and Their Computation by Means of Integral Equations," Boundary Problems in Differential Equations, Ed., R. E. Langer, University of Wisconsin Press, Madison, WI, 1960.

18. Tada, H., Paris, P. C., and Irwin, G. R., The Stress Analysis of Cracks Handbook, Del Research Corporation, Hellertown, PA, 1973.

19. Benthem, J. P. and Koiter, W. T., Asymptotic Approximations to Crack Problems," Methods of Analysis of Crack Problems, Ed. G. C. Sih, Noordhoff International Publishing, 1972.

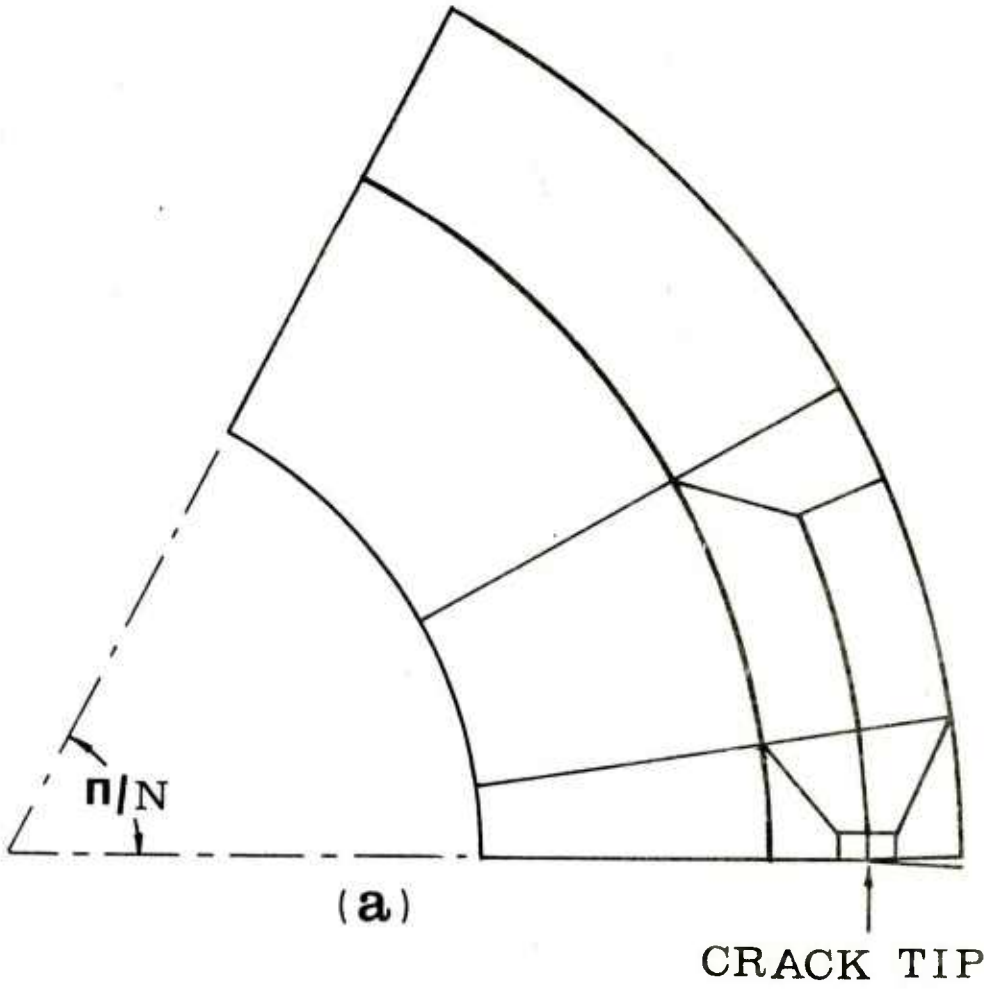

Figure 1(a). A typical finite element idealization.

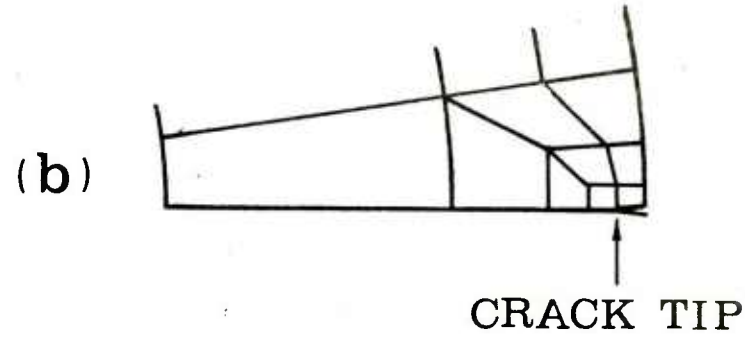

Figure 1(b). Idealization for very shallow cracks.

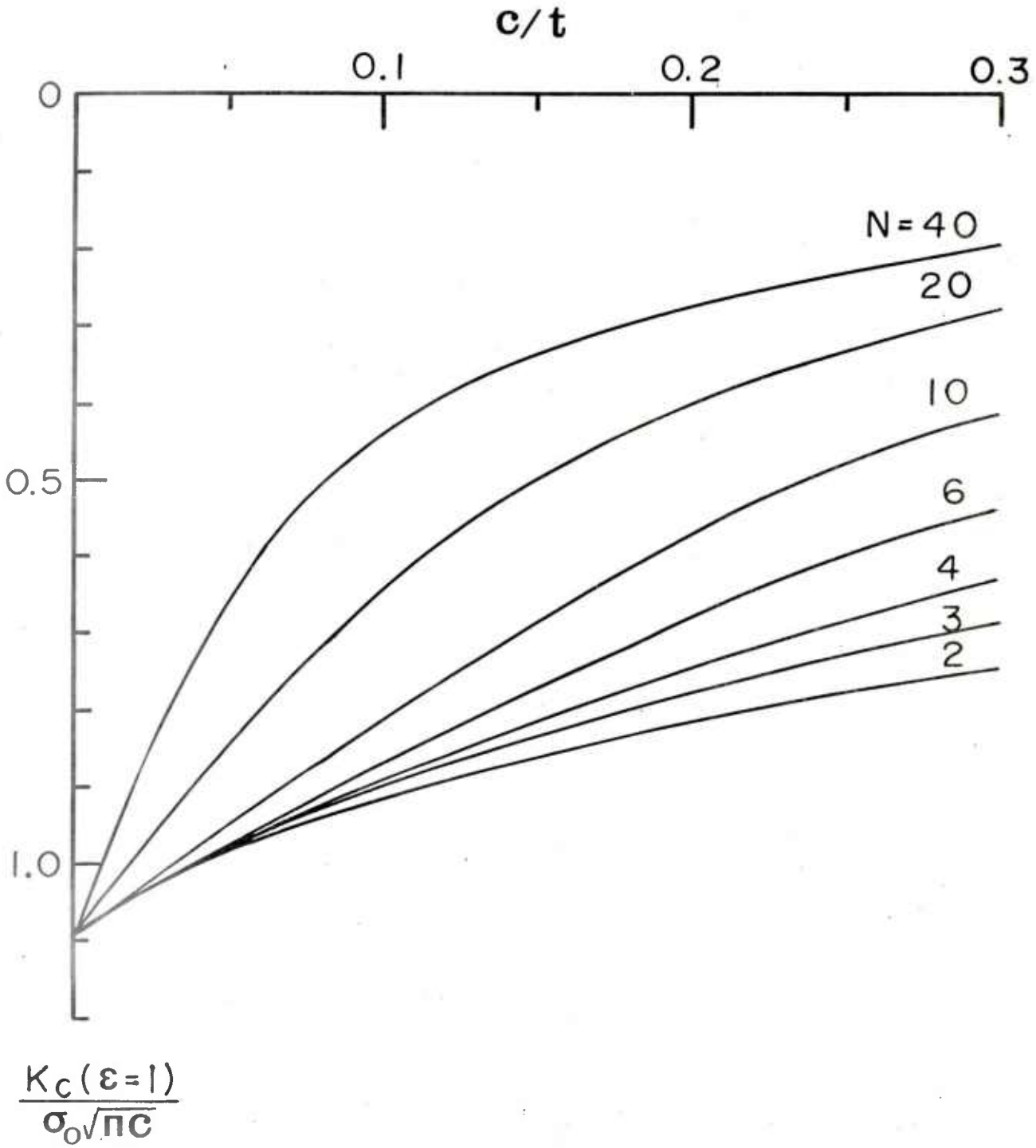

Figure 2. Stress intensity factor as a function of c/t for N ID cracks in a fully autofrettaged cylinder of b/a = 2.

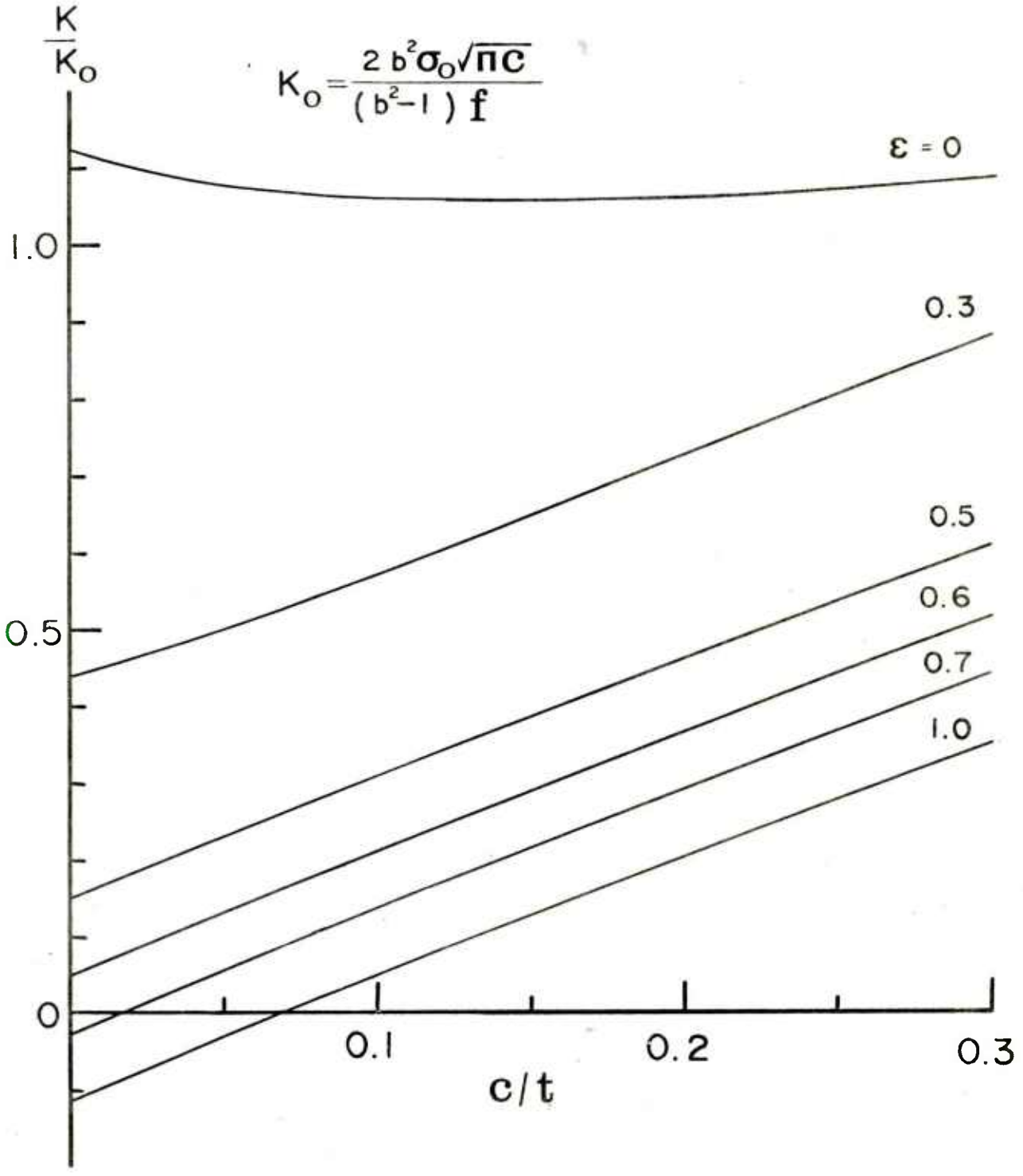

Figure 3. K/K_o as a function of c/t for a single crack at inner surface of a cylinder of b/a = 2 subjected to an internal pressure $p_i = \sigma_o/f$, f = 3, and residual stresses corresponding to various degrees of autofrettage, ε.

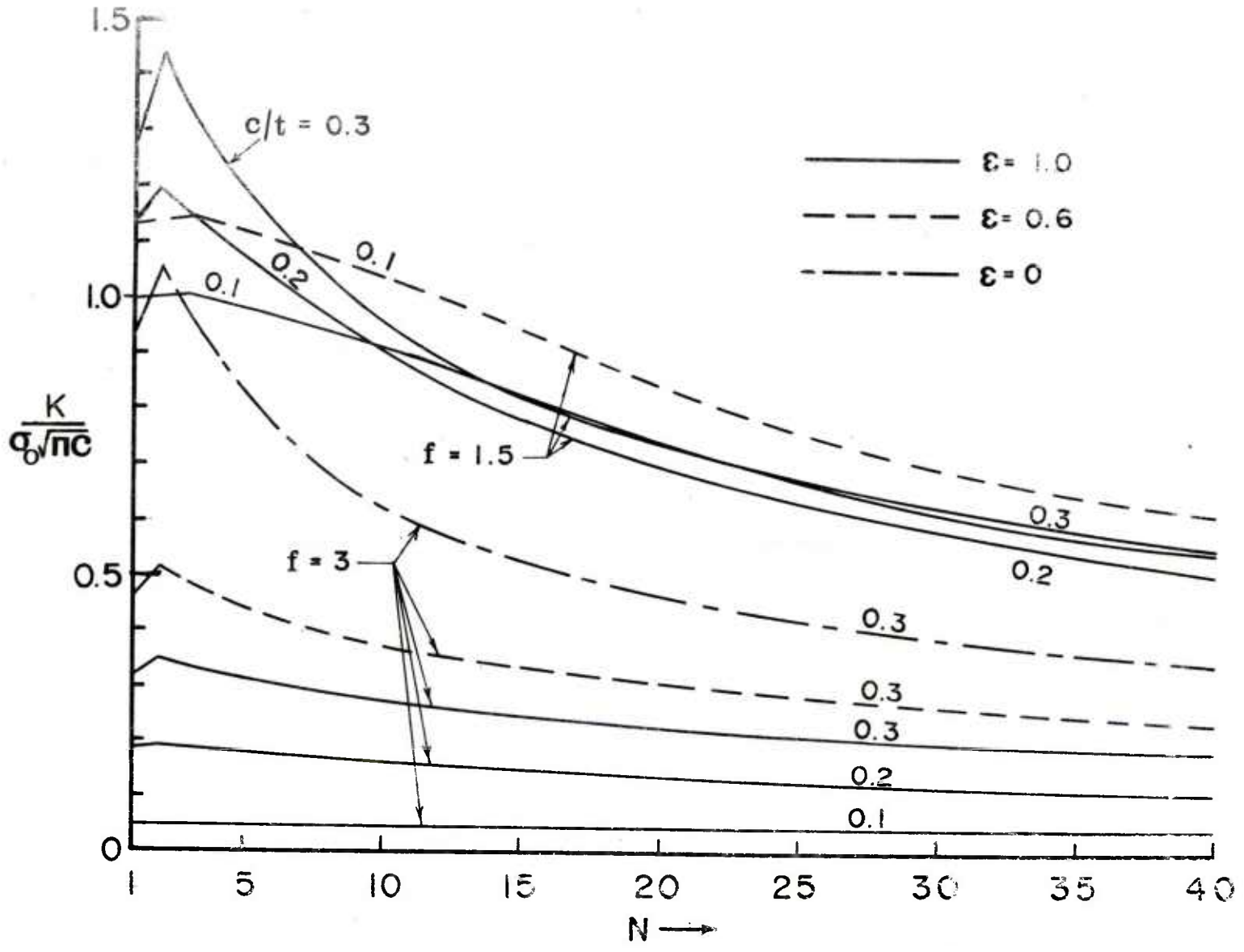

Figure 4. $K/\sigma_o\sqrt{\pi c}$ for N radial cracks at inner surface of a cylinder of b/a = 2 subjected to combined internal pressure $p_i = \sigma_o/f$ and residual stresses corresponding to given degrees of autofrettage, ε.

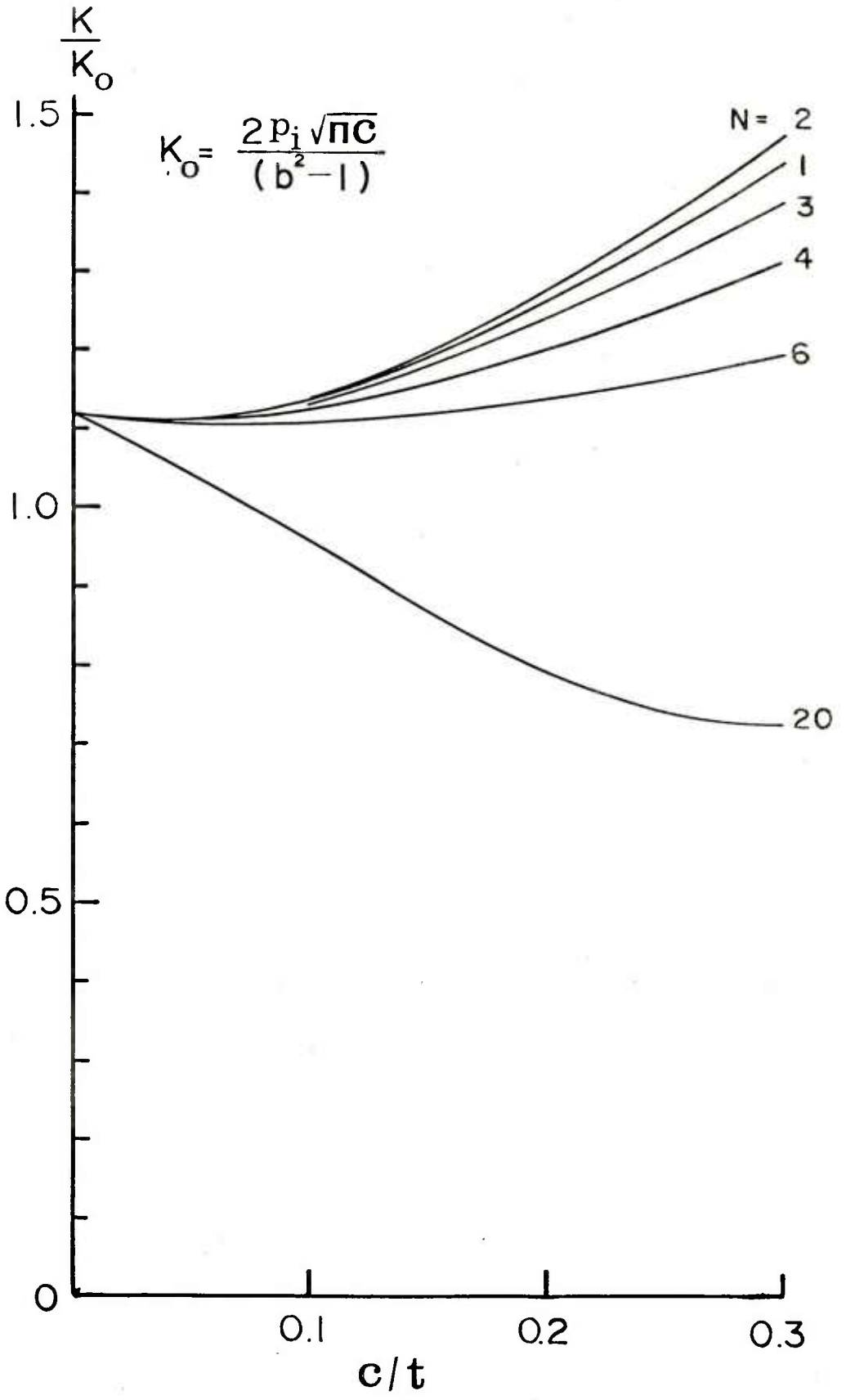

Figure 5. K/K_o as a function of c/t for N radial cracks at outer surface of a cylinder of b/a = 2 subjected to an internal pressure p_i.

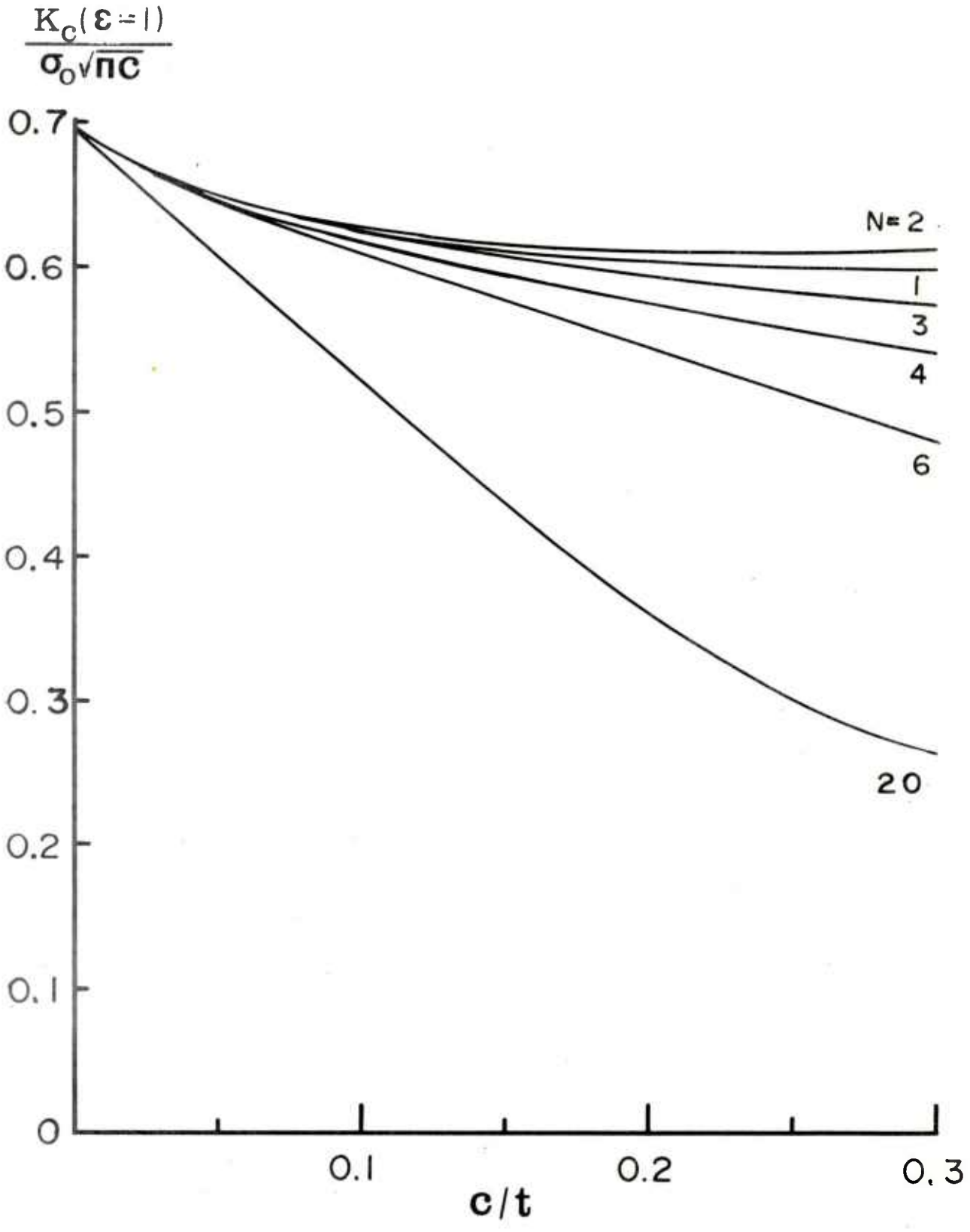

Figure 6. $K/\sigma_o\sqrt{\pi c}$ as a function of c/t for N radial cracks at outer surface of a fully autofrettaged cylinder of b/a = 2.

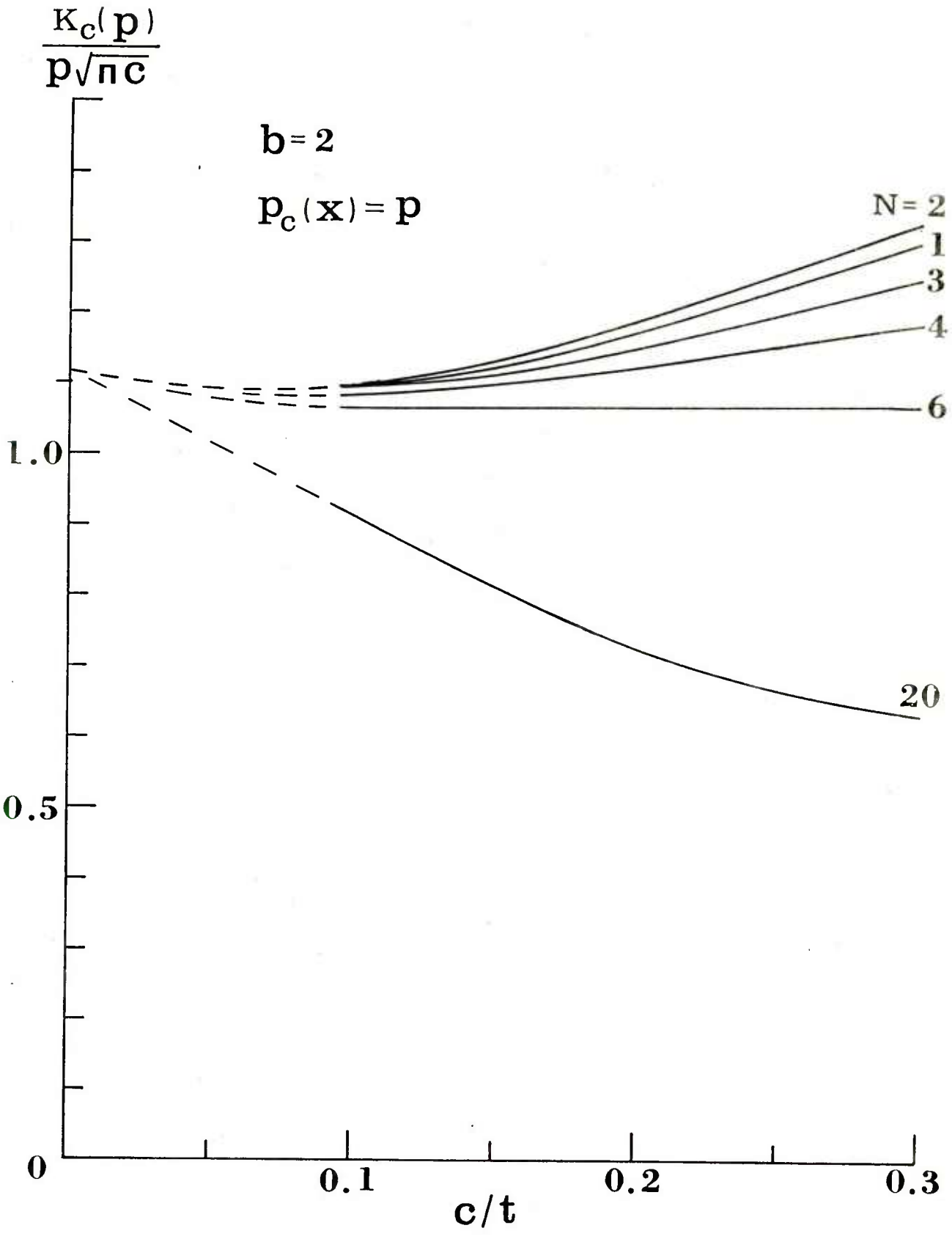

Figure 7. $K_c(p)/p\sqrt{\pi c}$ as a function of c/t for N external radial cracks with constant crack face loading.

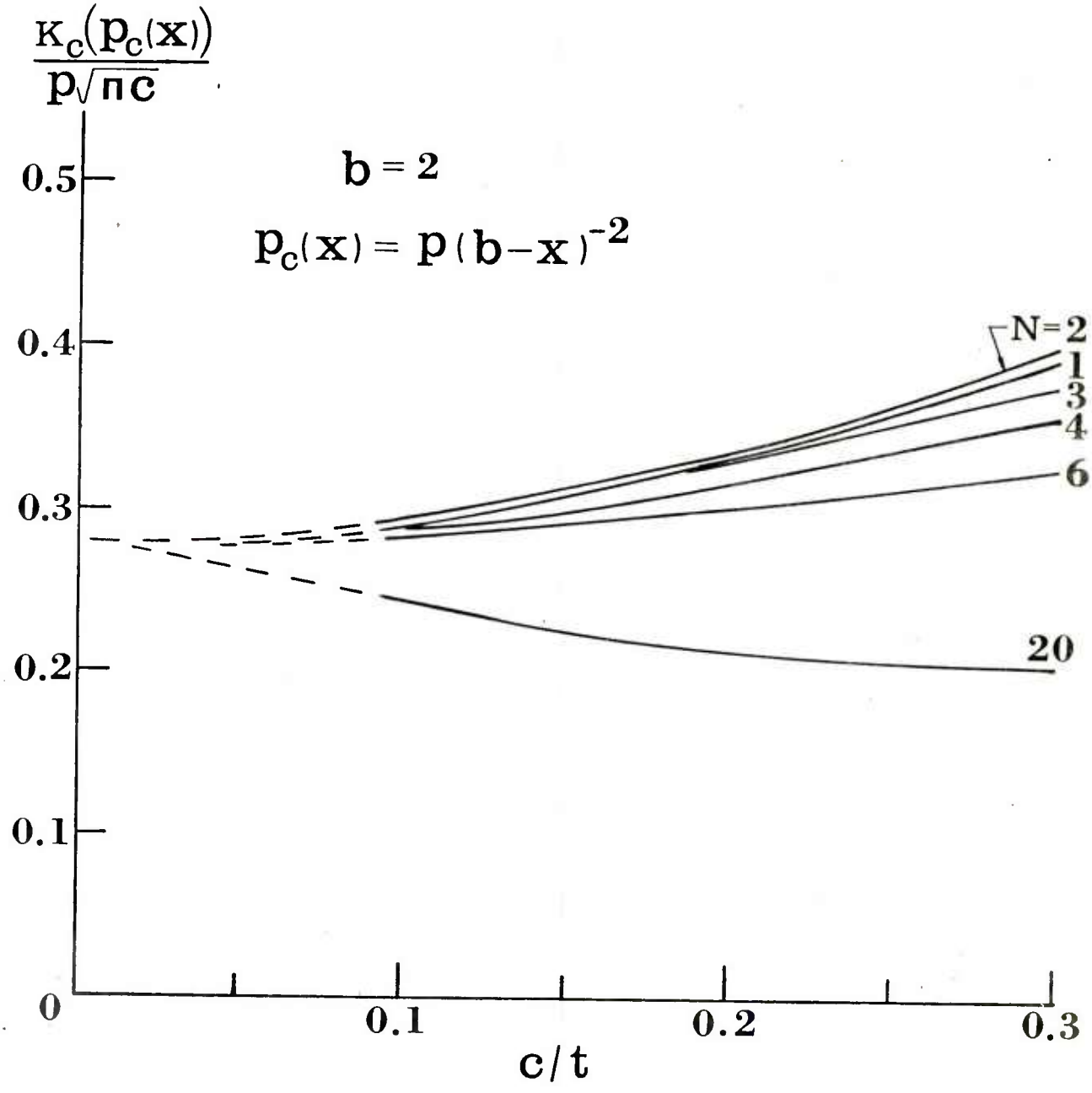

Figure 8. $K_c/p\sqrt{\pi c}$ vs. c/t for N external radial cracks with crack face loading $p_c(x) = p(b-x)^{-2}$.

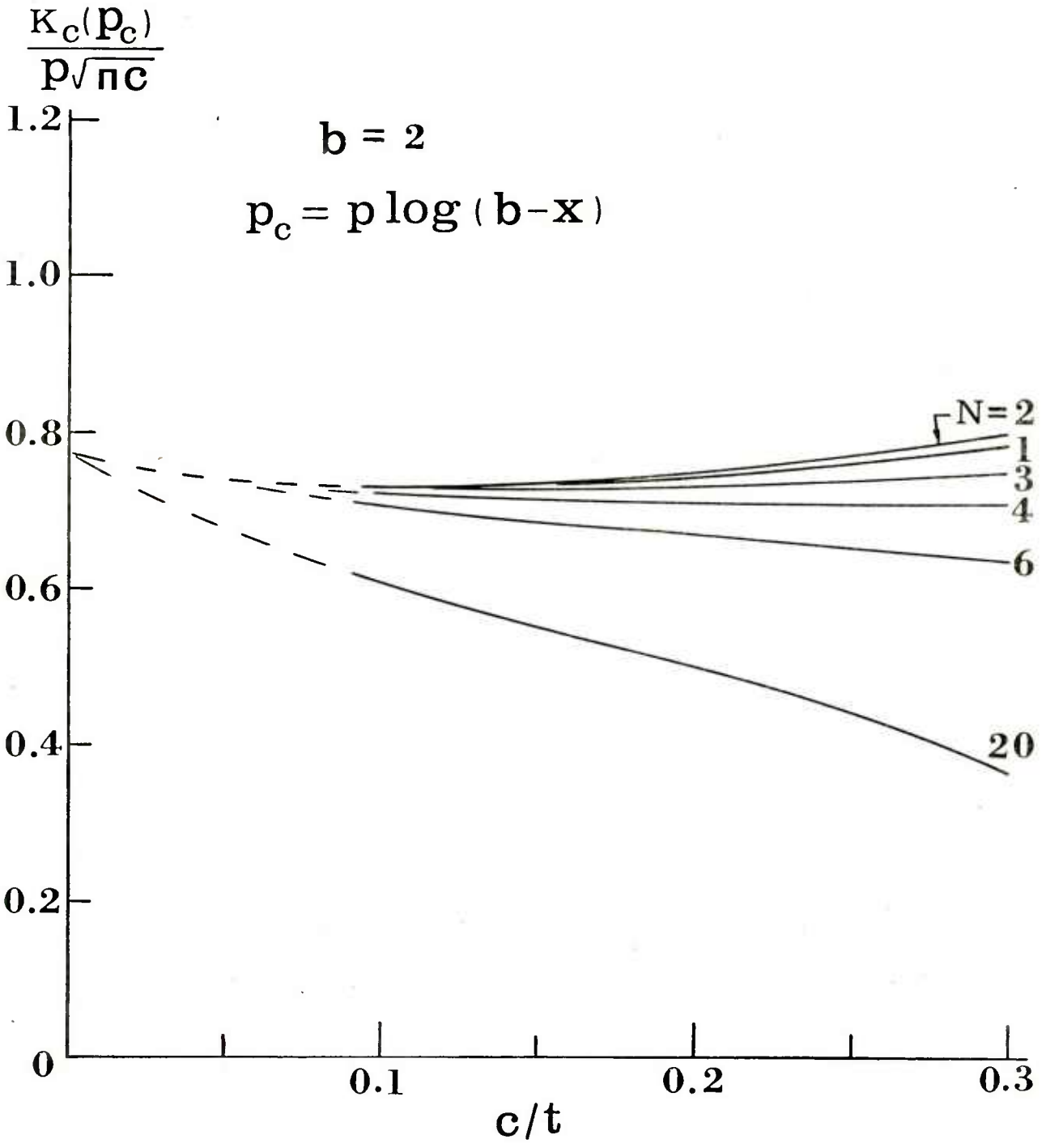

Figure 9. $K_c/p\sqrt{\pi c}$ vs. c/t for N external radial cracks with crack face loading $p_c(x) = p\log(b-x)$.

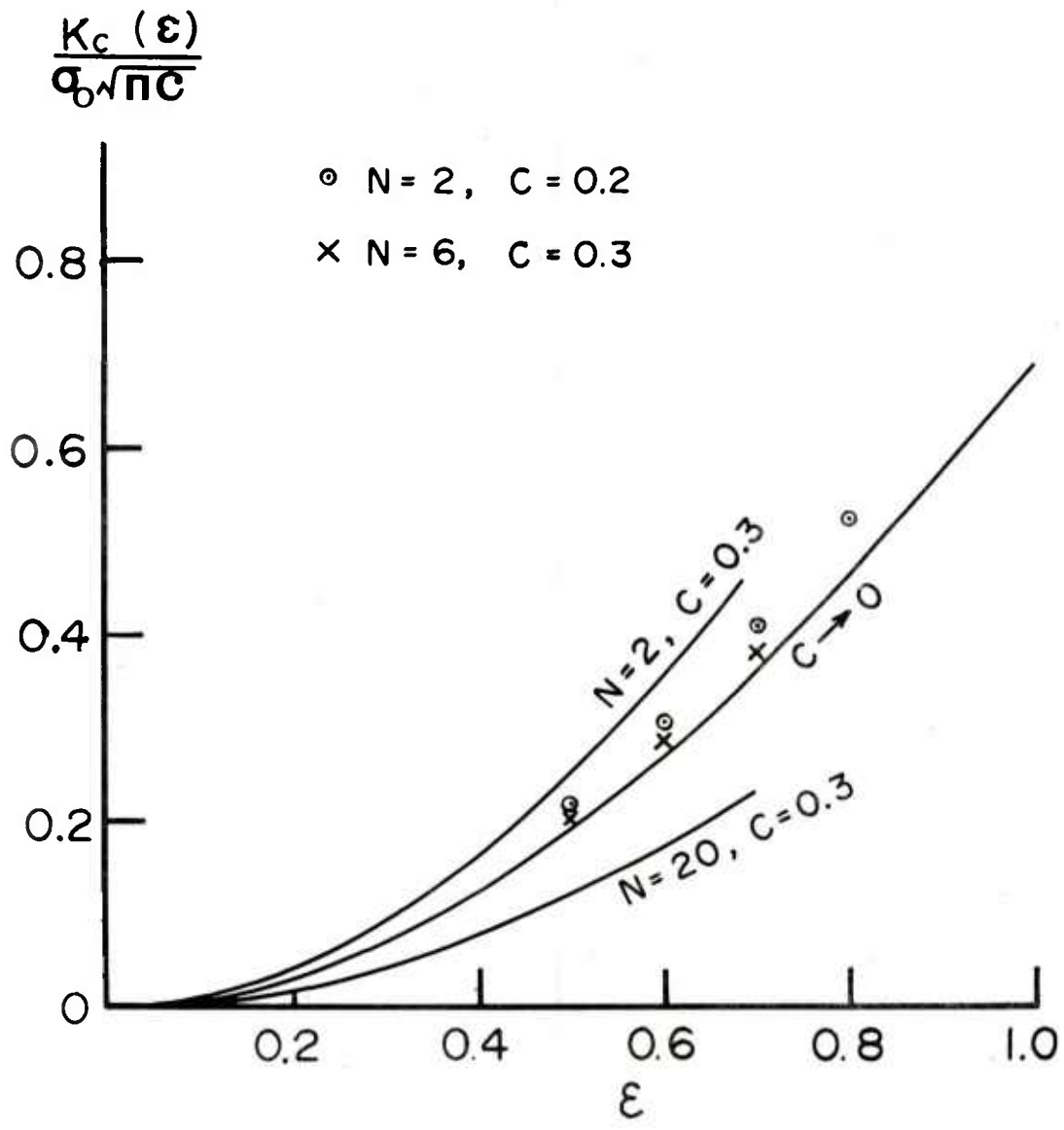

Figure 10. $K_c(\varepsilon)/\sigma_o\sqrt{\pi c}$ as a function of ε for a cylinder of b/a = 2 for several selected values of N and c (c = c/t since t = 1).

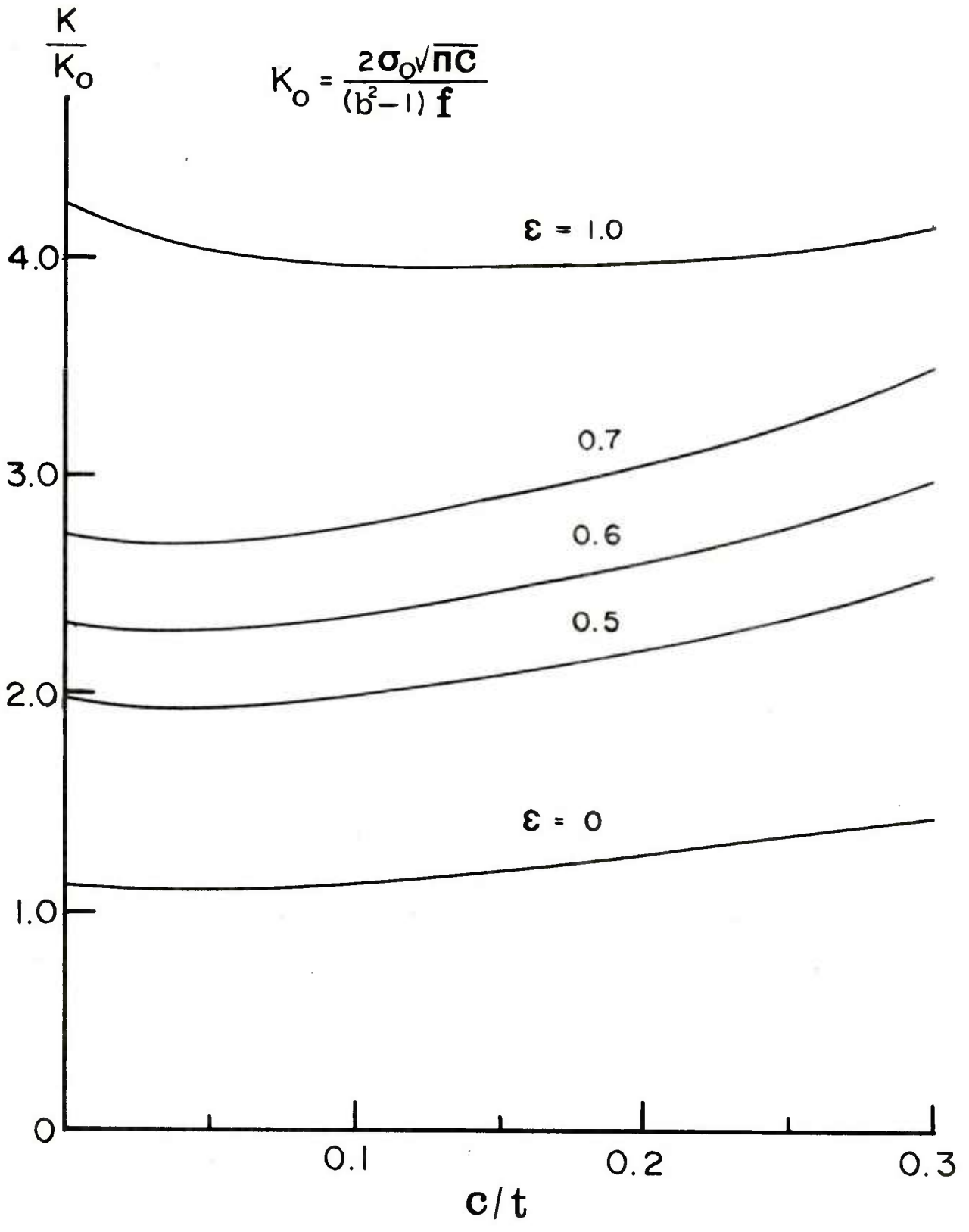

Figure 11. K/K_o as a function of c/t for a single externally cracked cylinder of b/a = 2 subjected to combined internal pressure $p_i = \sigma_o/f$, f = 3, and residual stresses corresponding to a degree of autofrettage ε given.

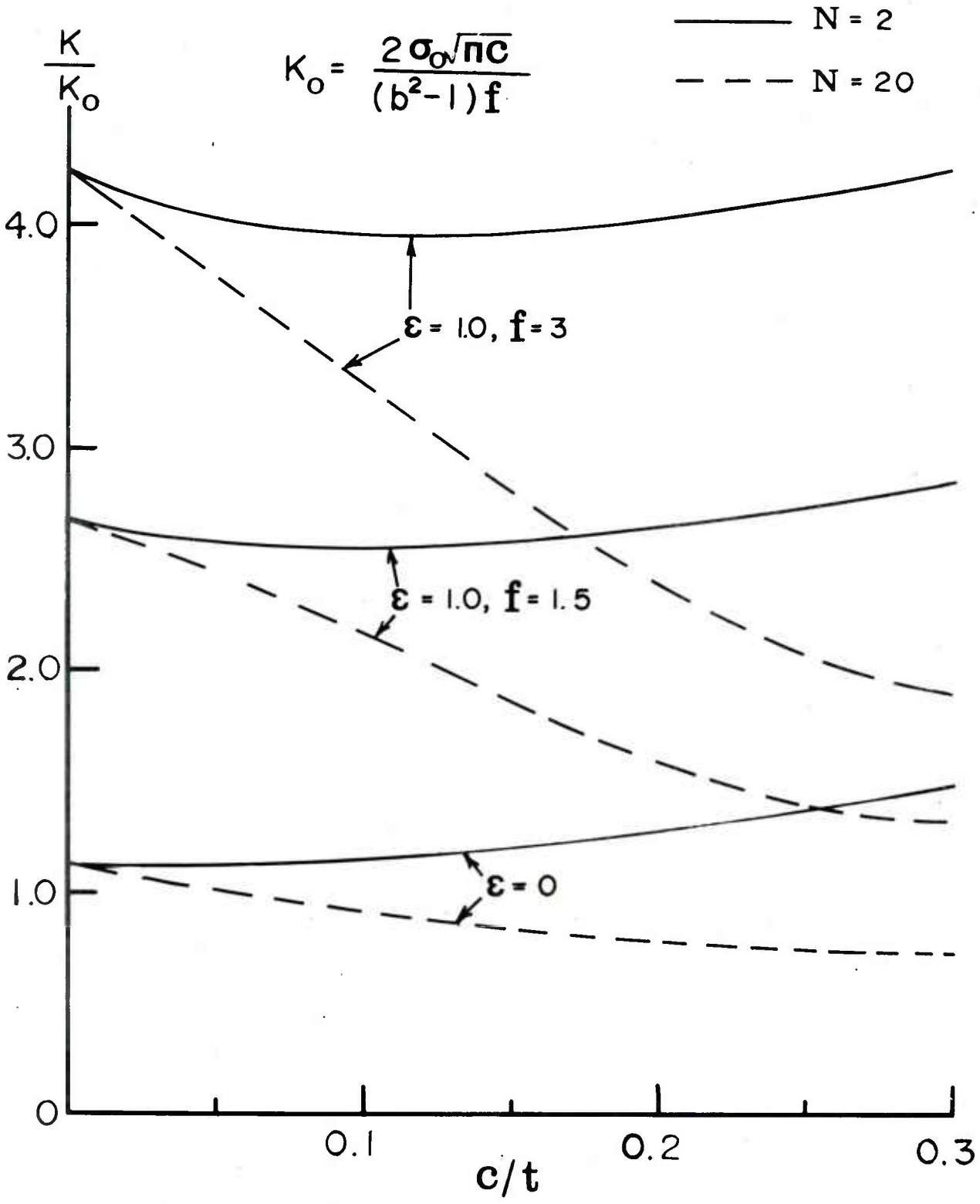

Figure 12. K/K_o as a function of c/t for N externally cracked cylinders of b/a = 2 subjected to several combinations of internal pressure $p_i = \sigma_o/f$ and residual stresses.

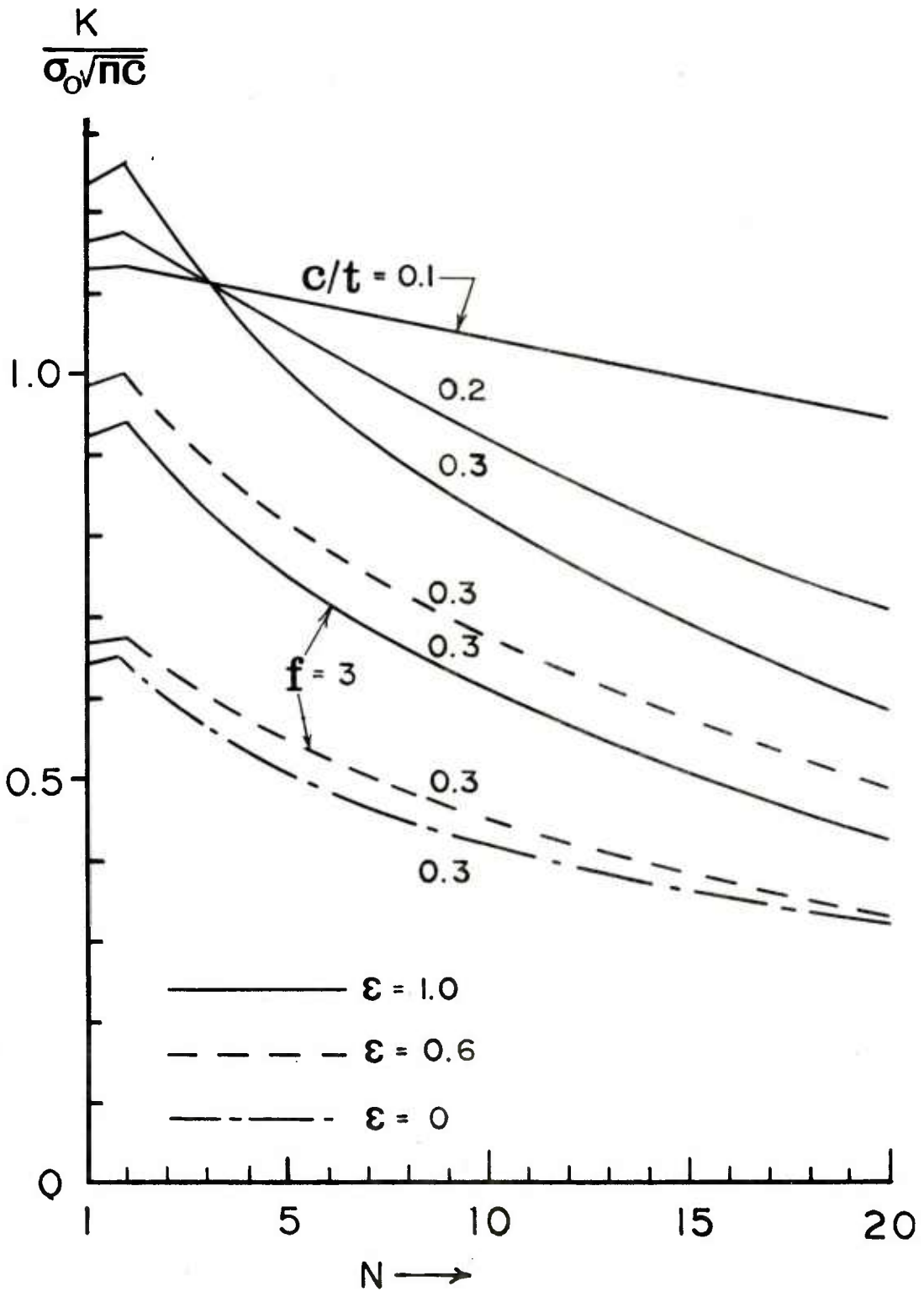

Figure 13. $K/\sigma_o\sqrt{\pi c}$ for N radial cracks at outer surface of a cylinder of $b/a = 2$ subjected to combined internal pressure $p_i = \sigma_o/f$, where $f = 1.5$ except otherwise indicated, and residual stresses corresponding to given degrees of autofrettage ε.

TECHNICAL REPORT INTERNAL DISTRIBUTION LIST

	NO. OF COPIES
COMMANDER	1
CHIEF, DEVELOPMENT ENGINEERING BRANCH	1
ATTN: DRDAR-LCB-DA	1
-DM	1
-DP	1
-DR	1
-DS (SYSTEMS)	1
-DS (ICAS GROUP)	1
-DC	1
CHIEF, ENGINEERING SUPPORT BRANCH	1
ATTN: DRDAR-LCB-SE	1
-SA	1
CHIEF, RESEARCH BRANCH	2
ATTN: DRDAR-LCB-RA	1
-RC	1
-RM	1
-RP	1
TECHNICAL LIBRARY	5
ATTN: DRDAR-LCB-TL	
TECHNICAL PUBLICATIONS & EDITING UNIT	2
ATTN: DRDAR-LCB-TL	
DIRECTOR, OPERATIONS DIRECTORATE	1
DIRECTOR, PROCUREMENT DIRECTORATE	1
DIRECTOR, PRODUCT ASSURANCE DIRECTORATE	1

NOTE: PLEASE NOTIFY DIRECTOR, BENET WEAPONS LABORATORY, ATTN: DRDAR-LCB-TL, OF ANY REQUIRED CHANGES.

TECHNICAL REPORT EXTERNAL DISTRIBUTION LIST

	NO. OF COPIES
ASST SEC OF THE ARMY RESEARCH & DEVELOPMENT ATTN: DEP FOR SCI & TECH THE PENTAGON WASHINGTON, D.C. 20315	1
COMMANDER US ARMY MAT DEV & READ. COMD ATTN: DRCDE 5001 EISENHOWER AVE ALEXANDRIA, VA 22333	1
COMMANDER US ARMY ARRADCOM ATTN: DRDAR-LC -LCA (PLASTICS TECH EVAL CEN) -LCE -LCM -LCS -LCW -TSS (STINFO) DOVER, NJ 07801	1 1 1 1 1 1 2
COMMANDER US ARMY ARRCOM ATTN: DRSAR-LEP-L ROCK ISLAND ARSENAL ROCK ISLAND, IL 61299	1
DIRECTOR US ARMY BALLISTIC RESEARCH LABORATORY ATTN: DRDAR-TSB-S (STINFO) ABERDEEN PROVING GROUND, MD 21005	1
COMMANDER US ARMY ELECTRONICS COMD ATTN: TECH LIB FT MONMOUTH, NJ 07703	1
COMMANDER US ARMY MOBILITY EQUIP R&D COMD ATTN: TECH LIB FT BELVOIR, VA 22060	1
COMMANDER US ARMY TANK-AUTMV R&D COMD ATTN: TECH LIB - DRDTA-UL MAT LAB - DRDTA-RK WARREN, MICHIGAN 48090	1 1
COMMANDER US MILITARY ACADEMY ATTN: CHMN, MECH ENGR DEPT WEST POINT, NY 10996	1
US ARMY MISSILE COMD REDSTONE SCIENTIFIC INFO CEN ATTN: DOCUMENTS SECT, BLDG 4484 REDSTONE ARSENAL, AL 35898	2
COMMANDER REDSTONE ARSENAL ATTN: DRSMI-RRS -RSM ALABAMA 35809	1 1
COMMANDER ROCK ISLAND ARSENAL ATTN: SARRI-ENM (MAT SCI DIV) ROCK ISLAND, IL 61299	1
COMMANDER HQ, US ARMY AVN SCH ATTN: OFC OF THE LIBRARIAN FT RUCKER, ALABAMA 36362	1
COMMANDER US ARMY FGN SCIENCE & TECH CEN ATTN: DRXST-SD 220 7TH STREET, N.E. CHARLOTTESVILLE, VA 22901	1
COMMANDER US ARMY MATERIALS & MECHANICS RESEARCH CENTER ATTN: TECH LIB - DRXMR-PL WATERTOWN, MASS 02172	2

NOTE: PLEASE NOTIFY COMMANDER, ARRADCOM, ATTN: BENET WEAPONS LABORATORY, DRDAR-LCB-TL, WATERVLIET ARSENAL, WATERVLIET, N.Y. 12189, OF ANY REQUIRED CHANGES.

TECHNICAL REPORT EXTERNAL DISTRIBUTION LIST (CONT.)

	NO. OF COPIES
COMMANDER US ARMY RESEARCH OFFICE P.O. BOX 12211 RESEARCH TRIANGLE PARK, NC 27709	1
COMMANDER US ARMY HARRY DIAMOND LAB ATTN: TECH LIB 2800 POWDER MILL ROAD ADELPHIA, MD 20783	1
DIRECTOR US ARMY INDUSTRIAL BASE ENG ACT ATTN: DRXPE-MT ROCK ISLAND, IL 61299	1
CHIEF, MATERIALS BRANCH US ARMY R&S GROUP, EUR BOX 65, FPO N.Y. 09510	1
COMMANDER NAVAL SURFACE WEAPONS CEN ATTN: CHIEF, MAT SCIENCE DIV DAHLGREN, VA 22448	1
DIRECTOR US NAVAL RESEARCH LAB ATTN: DIR, MECH DIV CODE 26-27 (DOC LIB) WASHINGTON, D.C. 20375	1 1
NASA SCIENTIFIC & TECH INFO FAC P.O. BOX 8757, ATTN: ACQ BR BALTIMORE/WASHINGTON INTL AIRPORT MARYLAND 21240	1

	NO. OF COPIES
COMMANDER DEFENSE TECHNICAL INFO CENTER ATTN: DTIA-TCA CAMERON STATION ALEXANDRIA, VA 22314	12 (2-LTD)
METALS & CERAMICS INFO CEN BATTELLE COLUMBUS LAB 505 KING AVE COLUMBUS, OHIO 43201	1
MECHANICAL PROPERTIES DATA CTR BATTELLE COLUMBUS LAB 505 KING AVE COLUMBUS, OHIO 43201	1
MATERIEL SYSTEMS ANALYSIS ACTV ATTN: DRXSY-MP ABERDEEN PROVING GROUND MARYLAND 21005	1

NOTE: PLEASE NOTIFY COMMANDER, ARRADCOM, ATTN: BENET WEAPONS LABORATORY, DRDAR-LCB-TL, WATERVLIET ARSENAL, WATERVLIET, N.Y. 12189, OF ANY REQUIRED CHANGES.